Towards Fully-Resolved Particulate-Induced Transition Simulations for High-Speed Boundary-Layers with an Immersed Boundary Method

O. M. F. Browne[1], S. M. A. Al Hasnine[2] and C. Brehm[3]

[1]Postdoctoral Research Associate

[2]Graduate Student

[3]Assistant Professor

Mechanical Engineering, University of Kentucky, Lexington, USA

NASA Ames Seminar, October 3rd 2019

Collaborators and Funding

- Funding provided by Office of Naval Research under contract N00014-19-1-2223 with **Dr. Eric Marineau** as program manager is gratefully acknowledged. **PI for this project: Dr. Christoph Brehm (University of Kentucky)**, awarded in March 2019

- External collaborators through SBIR (AFOSR): **Prof. Hermann Fasel** (University of Arizona), **Anthony Haas** (University of Arizona),

- Fruitful discussions on particle modeling with **Prof. Anatoli Tumin** (University of Arizona)

- This research is part of the **Blue Waters** sustained-petascale computing project which is supported by the National Science Foundation (awards OCI-0725070 and ACI-1238993) and the state of Illinois. Blue Waters is a joint effort of the University of Illinois at Urbana-Champaign and its National Center for Supercomputing Applications,

Outline

Particle Flow Simulations Background

Background, prior research and findings.

Numerical Methods

BitCart, Dual-Mesh Approach, and AMR.

Simulations Results

Validation, and 2D/3D patricle flow simulations results.

Summary, Outlook, & Research Interest

Summary of presented research

Outline

Particle Flow Simulations Background

Background, prior research and findings.

Numerical Methods

BitCart, Dual-Mesh Approach, and AMR.

Simulations Results

Validation, and 2D/3D patricle flow simulations results.

Summary, Outlook, & Research Interest

Summary of presented research

Hypersonic Free Flight Disturbance Environment

- Understanding of the relevant physics is essential to **reduce design margins** and **systems uncertainties** and, ultimately, guide the development of novel innovative designs

Artist's concepts of hypersonic cruise hardware

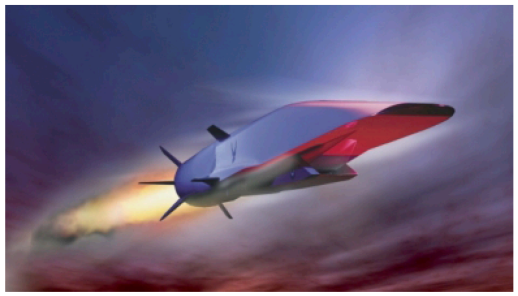

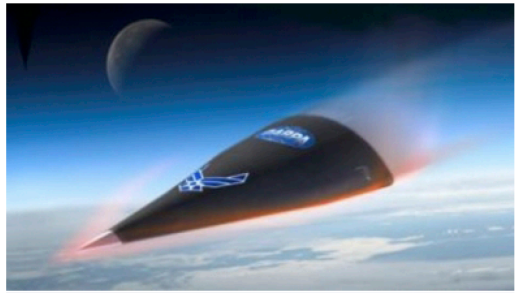

USAF

DARPA

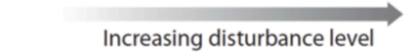

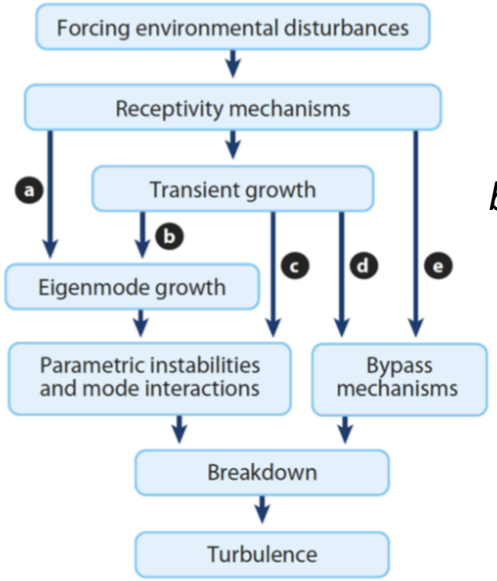

Paths to turbulence in boundary-layer flows

adapted from Morkovin et al. (1994)

Hypersonic Free Flight Disturbance Environment

- Understanding of the relevant physics is essential to **reduce design margins** and **systems uncertainties** and, ultimately, guide the development of novel innovative designs
- **Disturbance environment and its effects** on the flow field need to be understood to provide accurate predictions

Artist's concepts of hypersonic cruise hardware

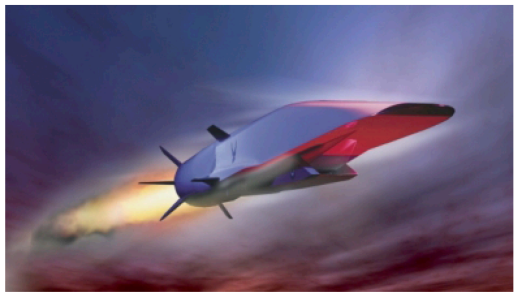

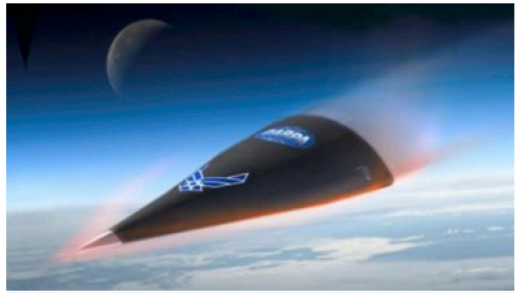

USAF

Increasing disturbance level

DARPA

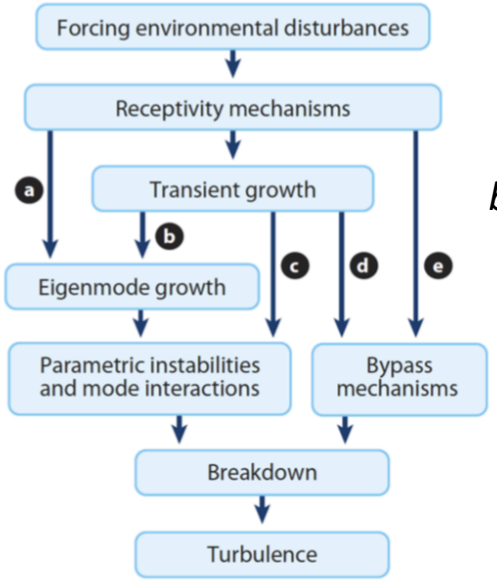

Paths to turbulence in boundary-layer flows

adapted from Morkovin et al. (1994)

Hypersonic Free Flight Disturbance Environment

- Understanding of the relevant physics is essential to **reduce design margins** and **systems uncertainties** and, ultimately, guide the development of novel innovative designs
- **Disturbance environment and its effects** on the flow field need to be understood to provide accurate predictions
- **Research Objective:** Provide physical insight into the interaction of the disturbance environment, in particular particulates, on the flow field during realistic high-speed flight conditions

Artist's concepts of hypersonic cruise hardware

USAF — DARPA

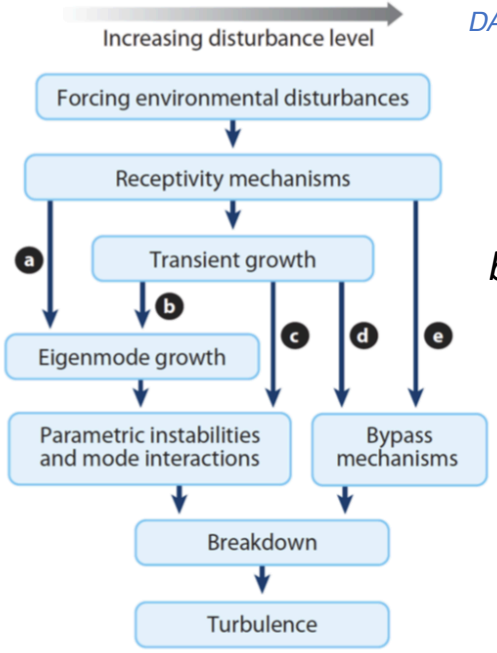

Paths to turbulence in boundary-layer flows

adapted from Morkovin et al. (1994)

Hypersonic Free Flight Disturbance Environment

- Understanding of the relevant physics is essential to **reduce design margins** and **systems uncertainties** and, ultimately, guide the development of novel innovative designs
- **Disturbance environment and its effects** on the flow field need to be understood to provide accurate predictions
- **<u>Research Objective:</u>** Provide physical insight into the interaction of the disturbance environment, in particular particulates, on the flow field during realistic high-speed flight conditions
- Consider **flow conditions (<u>cruise conditions</u>)** at altitude of **15-45 km** (stratosphere) with a free-stream temperature range of 217 to 260 K and free-stream Mach numbers between **4-18**

Artist's concepts of hypersonic cruise hardware

USAF — Increasing disturbance level — DARPA

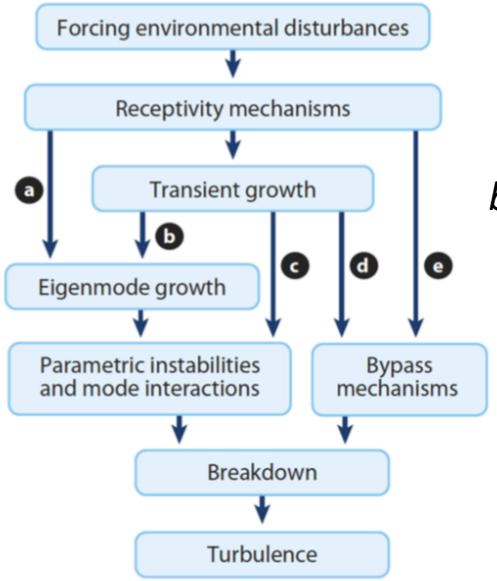

Paths to turbulence in boundary-layer flows

adapted from Morkovin et al. (1994)

Hypersonic Free Flight Disturbance Environment

- Understanding of the relevant physics is essential to **reduce design margins** and **systems uncertainties** and, ultimately, guide the development of novel innovative designs
- **Disturbance environment and its effects** on the flow field need to be understood to provide accurate predictions
- **Research Objective:** Provide physical insight into the interaction of the disturbance environment, in particular particulates, on the flow field during realistic high-speed flight conditions
- Consider **flow conditions (cruise conditions)** at altitude of **15-45 km** (stratosphere) with a free-stream temperature range of 217 to 260 K and free-stream Mach numbers between **4-18**

Artist's concepts of hypersonic cruise hardware

USAF DARPA

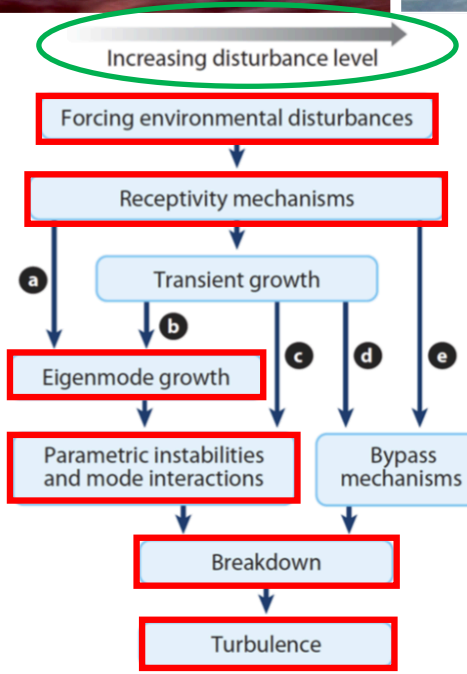

Paths to turbulence in boundary-layer flows

adapted from Morkovin et al. (1994)

Hypersonic Free Flight Disturbance Environment

Free flight disturbances environment ⟹ converted to instability waves via receptivity process

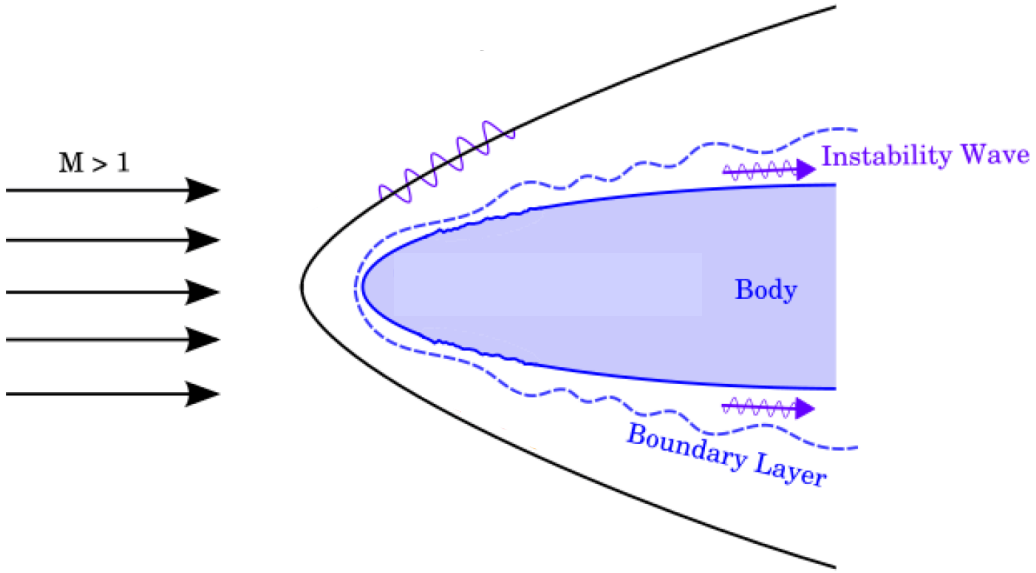

adapted from Zhong (1998)

Hypersonic Free Flight Disturbance Environment

Free flight disturbances environment ⟹ converted to instability waves via receptivity process

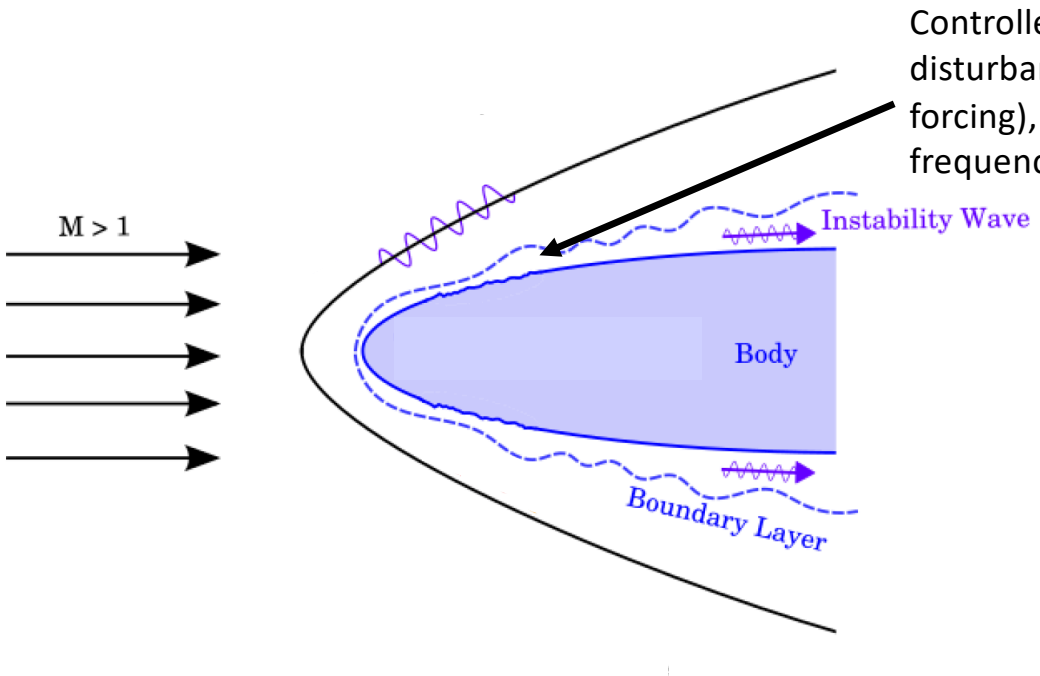

Controlled transition, wall disturbances (BC or volume forcing), defined amplitude and frequency/wavenumber band

adapted from Zhong (1998)

Hypersonic Free Flight Disturbance Environment

Free flight disturbances environment ⟹ converted to instability waves via receptivity process

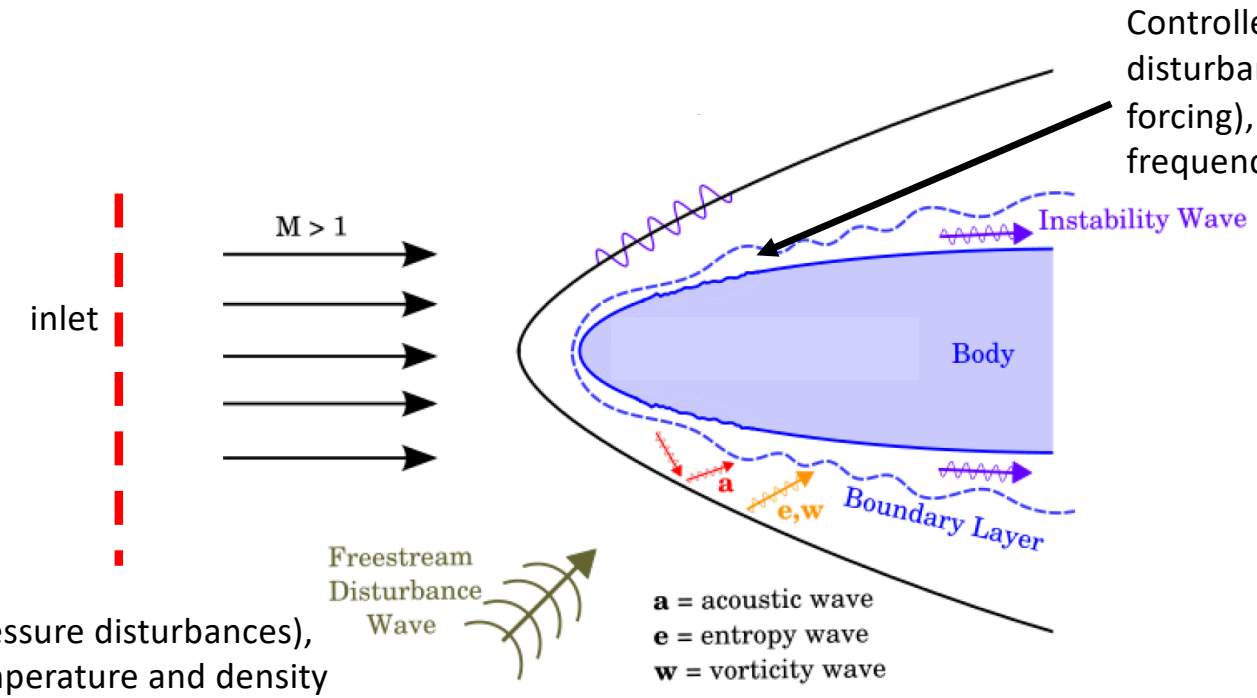

Controlled transition, wall disturbances (BC or volume forcing), defined amplitude and frequency/wavenumber band

adapted from Zhong (1998)

Acoustic waves (pressure disturbances), **entropy waves** (temperature and density disturbances), **vorticity waves** (turbulence). Introduced at or near BC inlet.

Hypersonic Free Flight Disturbance Environment

Free flight disturbances environment ⟹ converted to instability waves via receptivity process

Introduced via forcing term (random low amplitude noise), Edwards and Tumin (2018)

Controlled transition, wall disturbances (BC or volume forcing), defined amplitude and frequency/wavenumber band

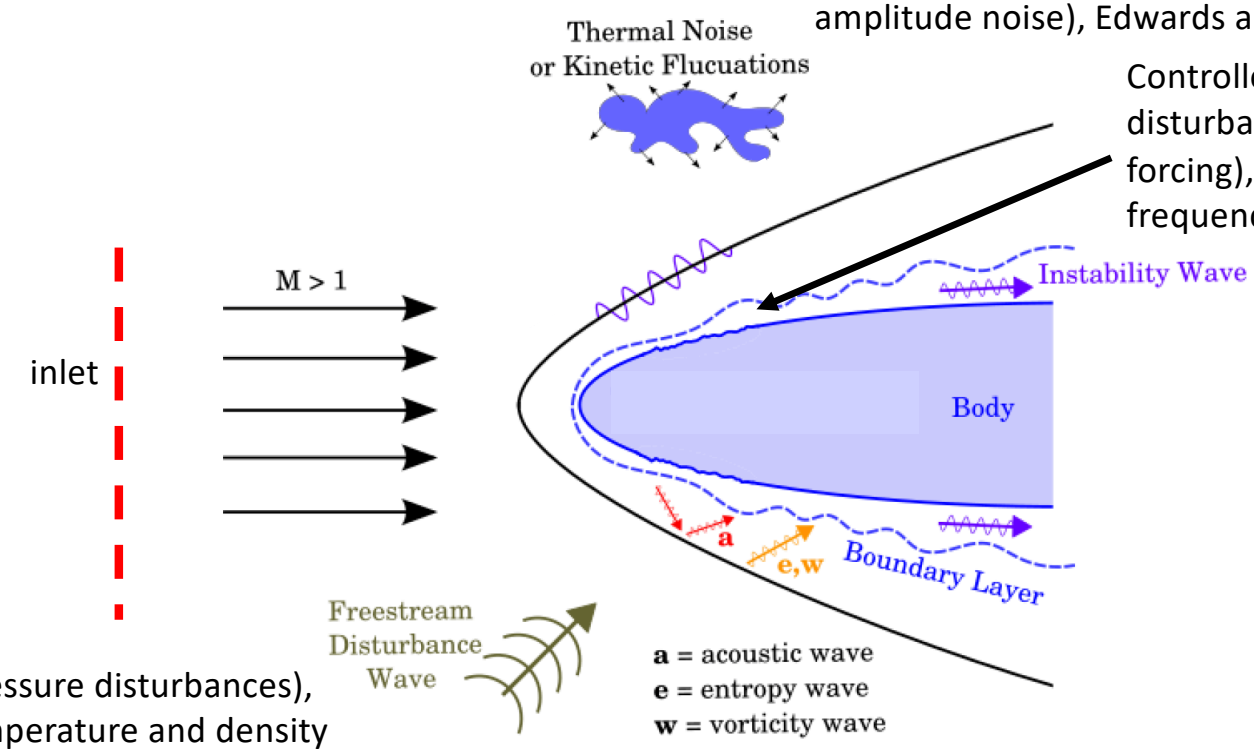

adapted from Zhong (1998)

Acoustic waves (pressure disturbances), **entropy waves** (temperature and density disturbances), **vorticity waves** (turbulence). Introduced at or near BC inlet.

Hypersonic Free Flight Disturbance Environment

Free flight disturbances environment ⟹ converted to instability waves via receptivity process

Introduced via forcing term (random low amplitude noise), Edwards and Tumin (2018)

Controlled transition, wall disturbances (BC or volume forcing), defined amplitude and frequency/wavenumber band

Isolated or distributed roughness (e.g. Schneider 2008), surface perturbations, body vibrations (couple CFD and CSD)

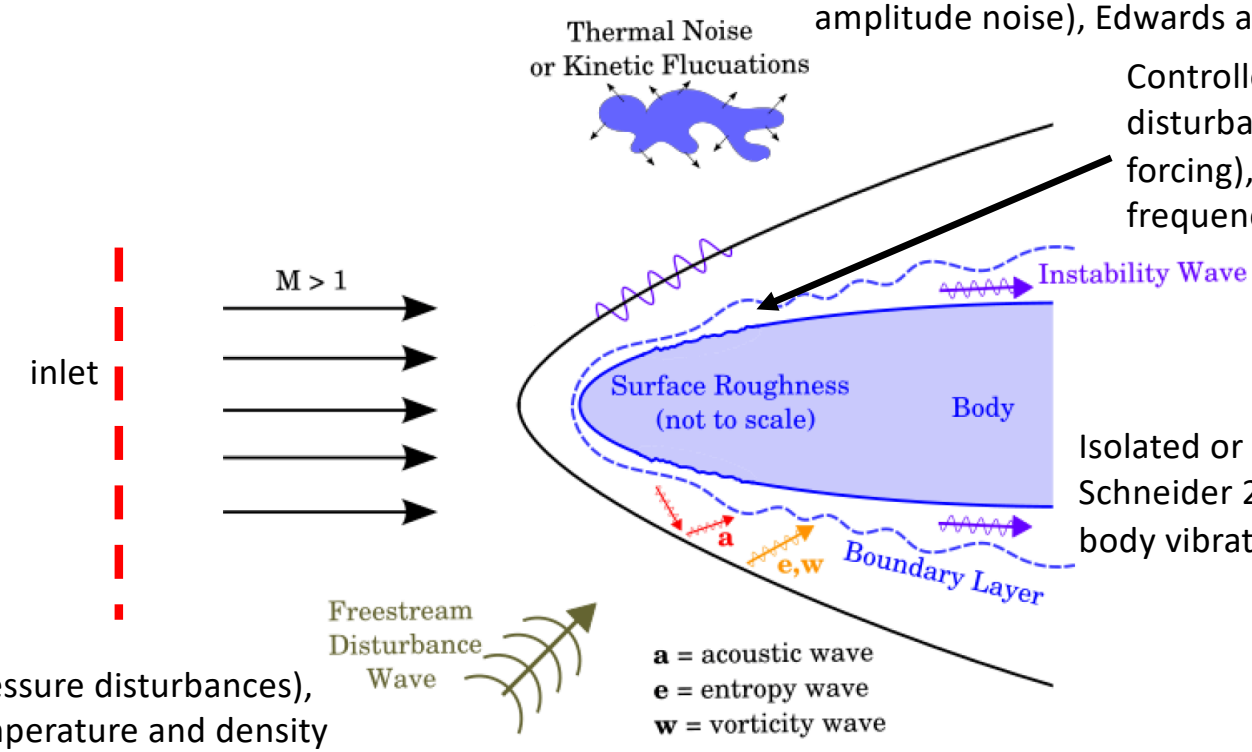

adapted from Zhong (1998)

Acoustic waves (pressure disturbances), **entropy waves** (temperature and density disturbances), **vorticity waves** (turbulence). Introduced at or near BC inlet.

Hypersonic Free Flight Disturbance Environment

Free flight disturbances environment ⟹ converted to instability waves via receptivity process

Introduced via acoustic beam in a forcing term, Malik et al. (1999)

Introduced via forcing term (random low amplitude noise), Edwards and Tumin (2018)

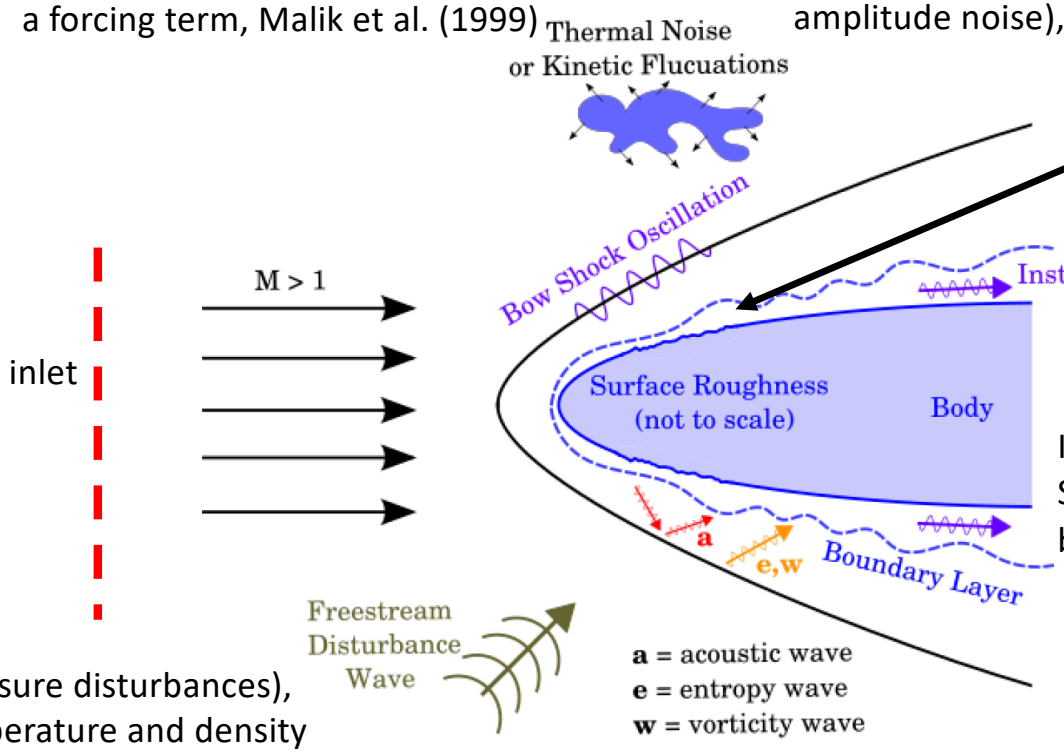

Controlled transition, wall disturbances (BC or volume forcing), defined amplitude and frequency/wavenumber band

Isolated or distributed roughness (e.g. Schneider 2008), surface perturbations, body vibrations (couple CFD and CSD)

Acoustic waves (pressure disturbances), **entropy waves** (temperature and density disturbances), **vorticity waves** (turbulence). Introduced at or near BC inlet.

adapted from Zhong (1998)

Hypersonic Free Flight Disturbance Environment

Free flight disturbances environment ⟹ converted to instability waves via receptivity process

Introduced via acoustic beam in a forcing term, Malik et al. (1999)

Introduced via forcing term (random low amplitude noise), Edwards and Tumin (2018)

Introduced via particle model or modeling particle. Fedorov (2013), Chuvakhov et al. (2019)

Controlled transition, wall disturbances (BC or volume forcing), defined amplitude and frequency/wavenumber band

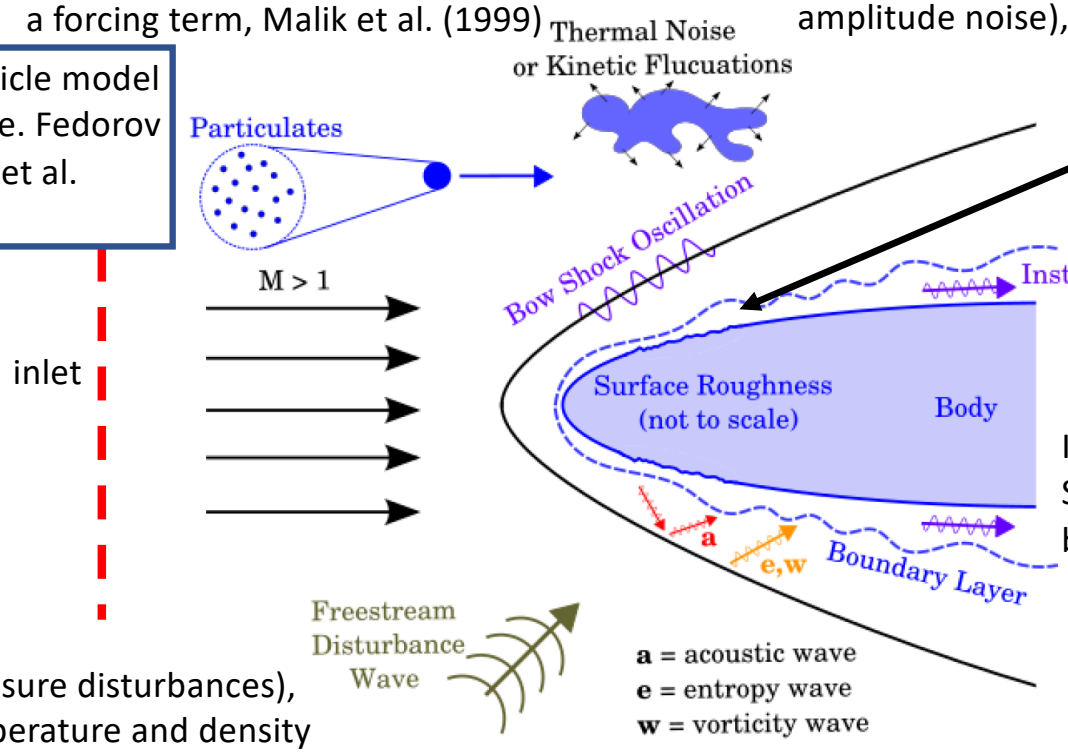

Isolated or distributed roughness (e.g. Schneider 2008), surface perturbations, body vibrations (couple CFD and CSD)

adapted from Zhong (1998)

Acoustic waves (pressure disturbances), **entropy waves** (temperature and density disturbances), **vorticity waves** (turbulence). Introduced at or near BC inlet.

Particle Properties in Atmosphere

- **Particulates are inevitably present** in the atmosphere as well as in wind tunnels (unless careful cleaning technique), and they can be a major source of disturbance energy
- Properties and concentration of particles in the atmosphere are documented in the literature (also see **Hypersonic Flight In the Turbulent Stratosphere Research Team at UCB**)
- **Highly variable and seasonably dependent**
- High concentration of particles can be obtained in **ice clouds** (mostly in troposphere, regular crystalline shaped $\mathcal{O}$(10-1000μm)))
- Large amount of particulates are related to **exhaust products from rockets** ($\mathcal{O}$(10μm))
- Another important source of particulates is **volcanic eruptions** ($\mathcal{O}$(1-20μm))

Approximate size distributions for particles with different origins in the Earth's middle atmosphere

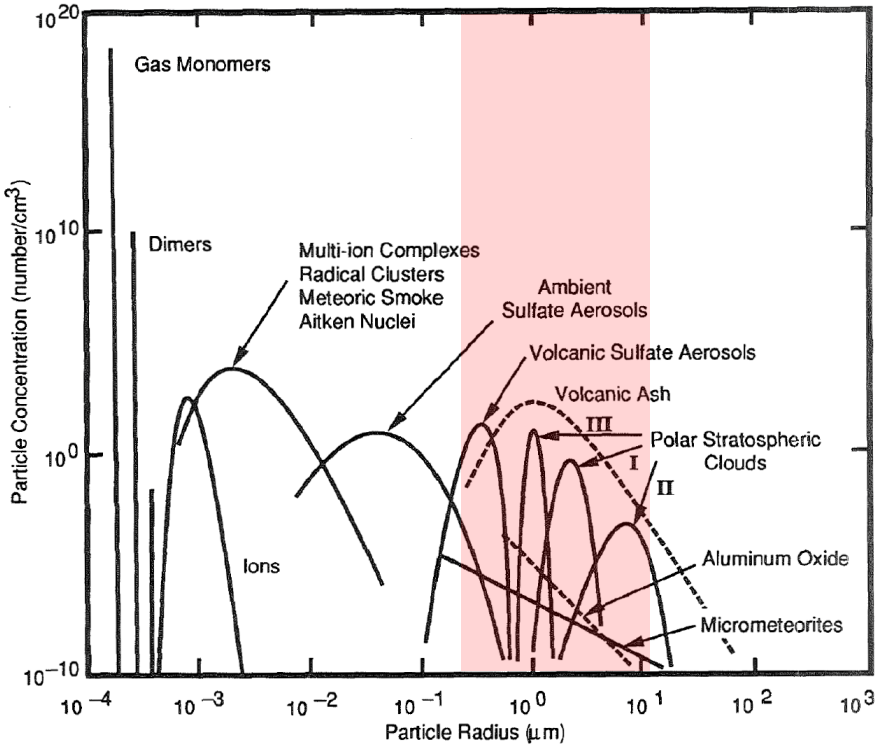

(adjusted from Turco, data before 1992)

Particle Properties in Atmosphere

- **Particulates are inevitably present** in the atmosphere as well as in wind tunnels (unless careful cleaning technique), and they can be a major source of disturbance energy
- Properties and concentration of particles in the atmosphere are documented in the literature (also see **Hypersonic Flight In the Turbulent Stratosphere Research Team at UCB**)
- **Highly variable and seasonably dependent**
- High concentration of particles can be obtained in **ice clouds** (mostly in troposphere, regular crystalline shaped $\mathcal{O}$(10-1000μm)))
- Large amount of particulates are related to **exhaust products from rockets** ($\mathcal{O}$(10μm))
- Another important source of particulates is **volcanic eruptions** ($\mathcal{O}$(1-20μm))

It is not a question of whether a flight vehicle encounters particles but rather how these particles affect the flow field around them!

Approximate size distributions for particles with different origins in the Earth's middle atmosphere

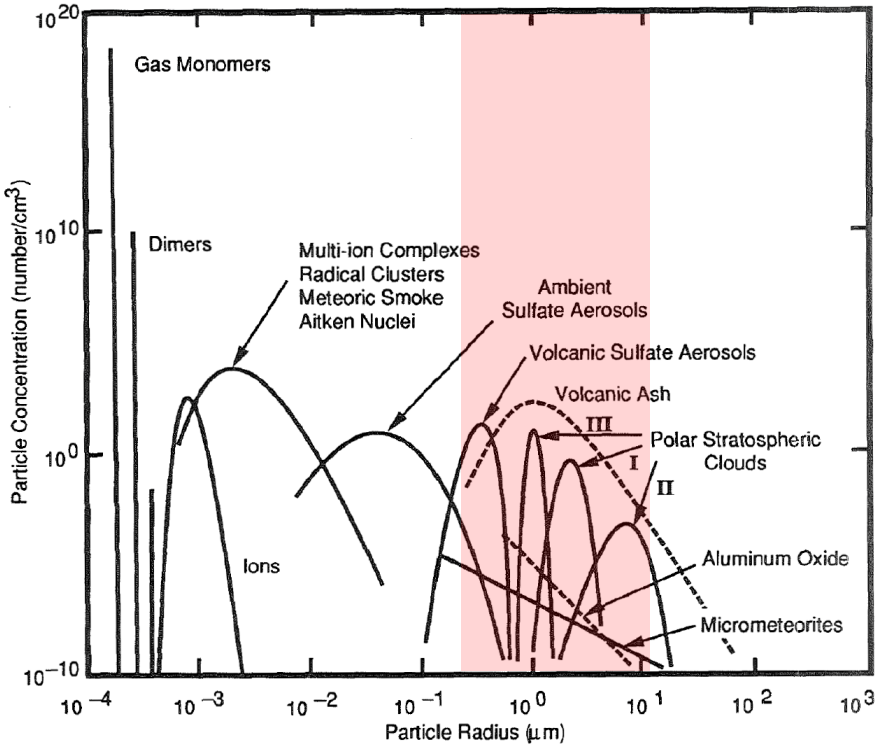

(adjusted from Turco, data before 1992)

Prior Research Studies & Findings

- **X-21 program** (conduct LFC wing studies) is a well-known example where **particle induced-transition** was relevant
  - during flight through light cirrus cloud and haze conditions at 25,000 feet (with 50 miles of visibility) laminar flow was lost [Bushnell 1990]

Prior Research Studies & Findings

- **X-21 program** (conduct LFC wing studies) is a well-known example where **particle induced-transition** was relevant
  - during flight through light cirrus cloud and haze conditions at 25,000 feet (with 50 miles of visibility) laminar flow was lost [Bushnell 1990]

JetStar configuration for LEFT program

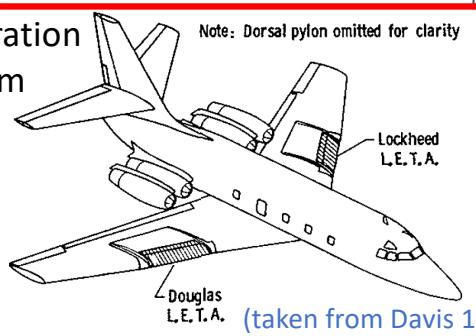

(taken from Davis 1986)

Predicted laminar flow degradation within clouds at 40kft and M=0.75 (for ice particles)

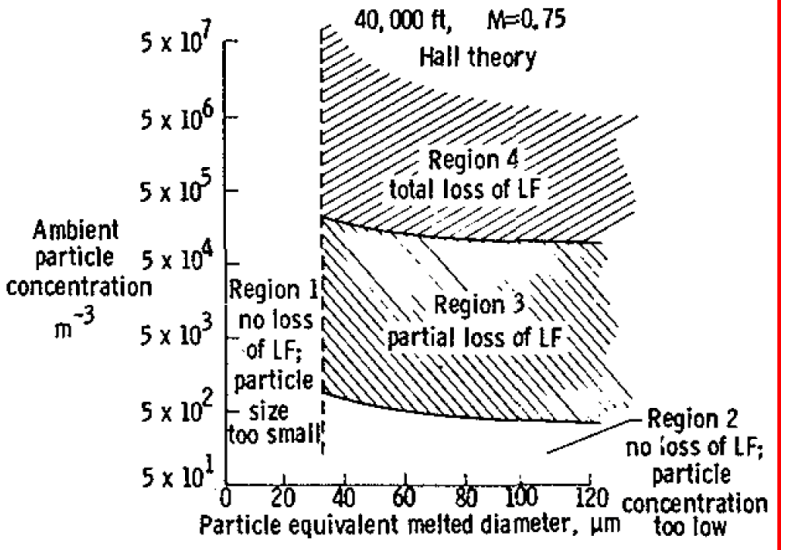

(taken from Davis 1986)

Prior Research Studies & Findings

- **X-21 program** (conduct LFC wing studies) is a well-known example where **particle induced-transition** was relevant
  - during flight through light cirrus cloud and haze conditions at 25,000 feet (with 50 miles of visibility) laminar flow was lost [Bushnell 1990]

- Transition mechanisms of **particles passing through an initially laminar boundary laye**r: [Hall, Davis (1986)]
  1) incident particles must have a **sufficient size** (or particle Reynolds number) to produce a turbulent spot
  2) particles must stay **inside the boundary layer for a sufficient time** to generate turbulence
  3) the **particle flux must be large enough** to result in a sufficiently large region of turbulent flow
  - ➢ **critical particle size** to cause transition was determined to be 17/34 microns at an altitude of 25,000 feet

- Atmospheric **particulates are capable of initiating laminar-turbulent transition** on aerodynamically smooth surfaces for high-speed vehicles [Fedorov 2018,Churakov 2019]

JetStar configuration for LEFT program

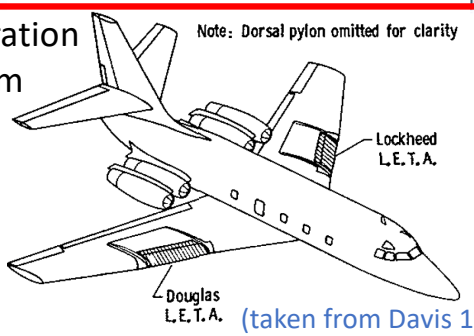

(taken from Davis 1986)

Predicted laminar flow degradation within clouds at 40kft and M=0.75 (for ice particles)

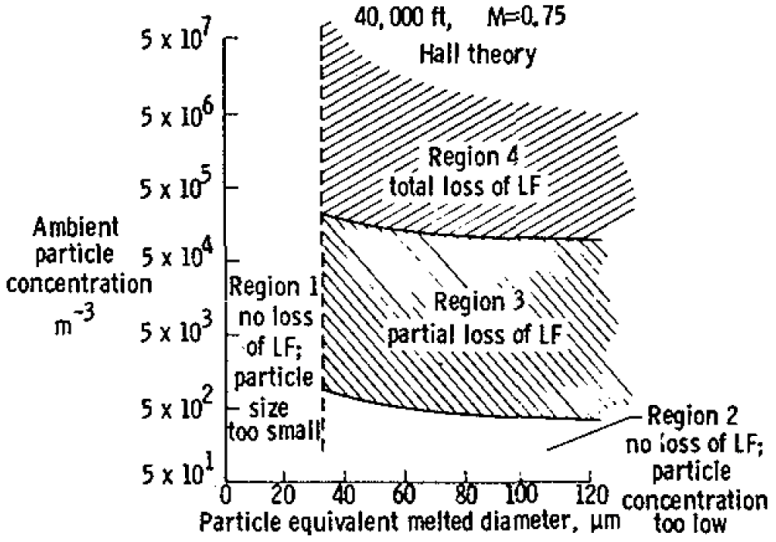

(taken from Davis 1986)

Particle Flow Interaction Mechanisms

Different mechanisms of how particles affect low and high-speed transition were summarized in Bushnell (1990):

1) **roughness** generation via impacting or sticking to the surface,

2) **vortex or vorticity shedding** when particle is immersed in or external to the boundary layer,

3) boundary-layer mean shear can cause **particle rotation and consequent fluid motions**,

4) "**reverse shocklets**" can occur when particle passes through the vehicle-induced shock, and

5) after particle impacts the surface it can rebound and **dynamically interact with the bow shock** induced by the vehicle causing the **formation of jets and shear-layers**.

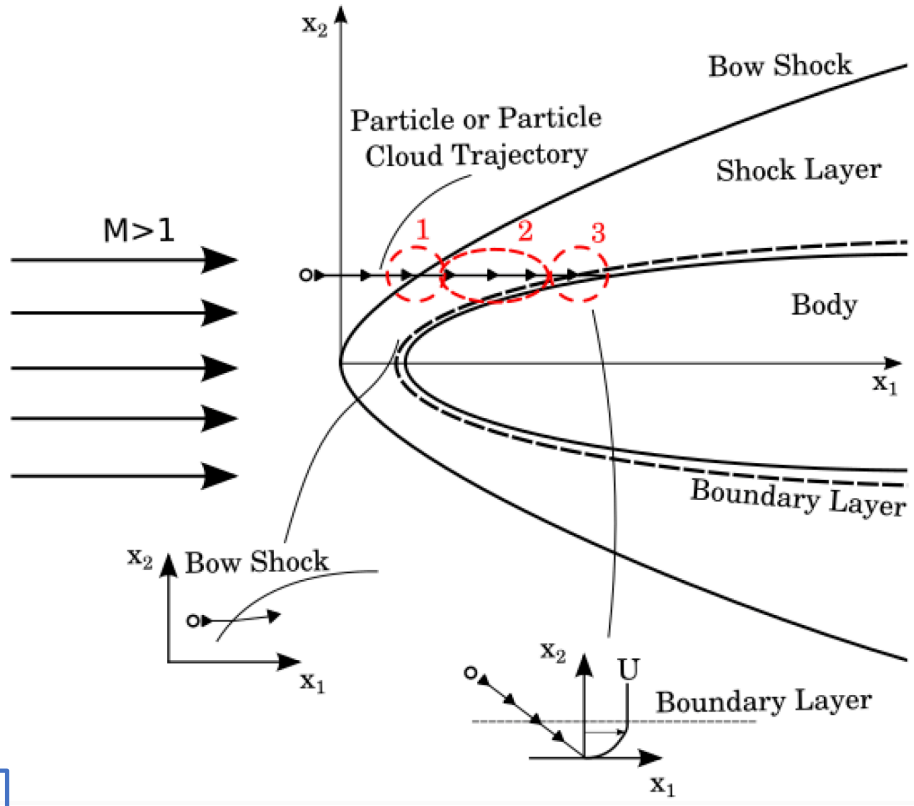

➢ **Not a complete list very few fundamental studies have been conducted, especially for hypersonic flow**.

“Develop numerical strategy for simulating particle flow induced instability waves/wavepackets for hypersonic transition prediction.”

Outline

Particle Flow Simulations Background

Background, prior research and findings.

Numerical Methods

BitCart, Dual-Mesh Approach, and AMR.

Simulations Results

Validation, and 2D/3D patricle flow simulations results.

Summary, Outlook, & Research Interest

Summary of presented research

Solver Overview & Simulation Approach

- **Compressible Navier-Stokes equations with in-house multi-physics solver *BitCart* *(developed at UK/UA/AZES)***
  - Conservative FD scheme
  - **Higher-order shock capturing (CWENO-6) for convective terms**
  - 4^{th}-order accurate treatment of viscous terms
  - Higher-order explicit and implicit time-discretization
  - **Higher-order immersed boundary method (IBM)**
  - Multi-species, gas chemistry, multi-phase, etc.
  - Fluid-structure interaction (FEM CSD solver)
  - Particle solver
  - Grid: generalized curvilinear, block-structured**, adaptive mesh refinement (AMR) Cartesian, dual-mesh overset**

Simulation Domain

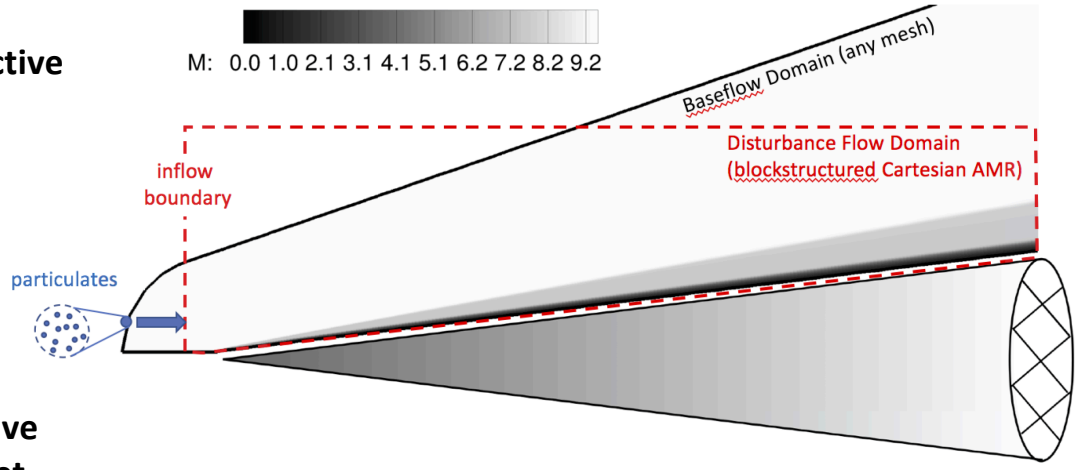

- DNS of particle flows: **solve nonlinear disturbance equations with IBM, AMR, and dual-mesh approach**

Solver Overview & Simulation Approach

- **Compressible Navier-Stokes equations with in-house multi-physics solver *BitCart* *(developed at UK/UA/AZES)***
  - Conservative FD scheme
  - **Higher-order shock capturing (CWENO-6) for convective terms**
  - 4^{th}-order accurate treatment of viscous terms
  - Higher-order explicit and implicit time-discretization
  - **Higher-order immersed boundary method (IBM)**
  - Multi-species, gas chemistry, multi-phase, etc.
  - Fluid-structure interaction (FEM CSD solver)
  - Particle solver
  - Grid: generalized curvilinear, block-structured**, adaptive mesh refinement (AMR) Cartesian, dual-mesh overset**

Simulation Domain

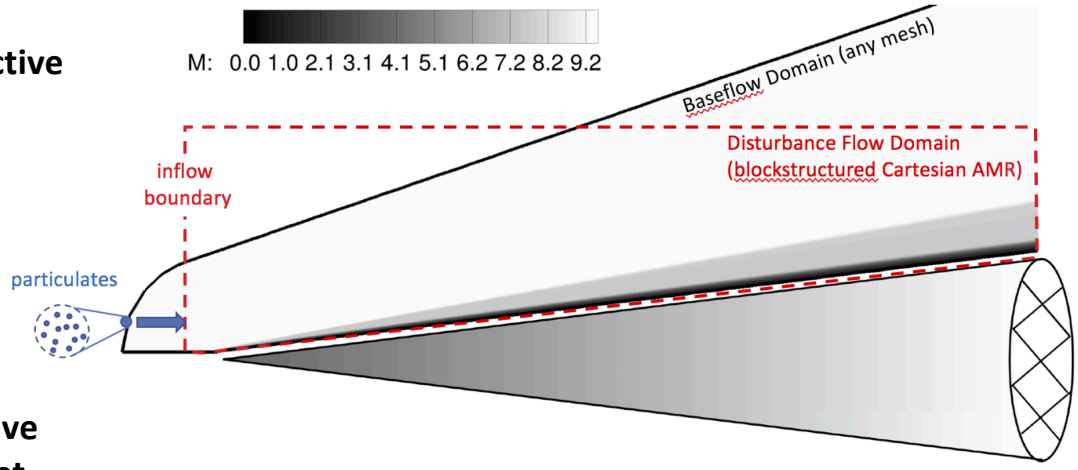

- DNS of particle flows: **solve nonlinear disturbance equations with IBM, AMR, and dual-mesh approach**

- **AMR-WPT: Motivation was to develop method that has fidelity of DNS but at a reduced computational cost.**

Nonlinear Disturbance Flow Formulation: NLDE

$$\frac{\partial \mathbf{W}}{\partial t} + \frac{\partial \mathbf{F}}{\partial x} + \frac{\partial \mathbf{G}}{\partial y} + \frac{\partial \mathbf{H}}{\partial z} = 0,$$

3D Compressible N.S. in vector form

Nonlinear Disturbance Flow Formulation: NLDE

$$\frac{\partial \mathbf{W}}{\partial t} + \frac{\partial \mathbf{F}}{\partial x} + \frac{\partial \mathbf{G}}{\partial y} + \frac{\partial \mathbf{H}}{\partial z} = 0,$$

3D Compressible N.S. in vector form

$$\mathbf{W} = \bar{\mathbf{W}} + \tilde{\mathbf{W}} = \bar{\mathbf{W}} + \tilde{\mathbf{W}}_l + \tilde{\mathbf{W}}_{nl} = \underbrace{\begin{bmatrix} \bar{\rho} \\ \bar{\rho}\bar{u} \\ \bar{\rho}\bar{v} \\ \bar{\rho}\bar{w} \\ \bar{\rho}\bar{E}_t \end{bmatrix}}_{\text{baseflow}} + \underbrace{\begin{bmatrix} \tilde{\rho} \\ \tilde{\rho}\bar{u} + \bar{\rho}\tilde{u} \\ \tilde{\rho}\bar{v} + \bar{\rho}\tilde{v} \\ \tilde{\rho}\bar{w} + \bar{\rho}\tilde{w} \\ \bar{\rho}\tilde{E}_t + \tilde{\rho}\bar{E}_t \end{bmatrix}}_{\text{linear disturbance}} + \underbrace{\begin{bmatrix} \\ \tilde{\rho}\tilde{u} \\ \tilde{\rho}\tilde{v} \\ \tilde{\rho}\tilde{w} \\ \tilde{\rho}\tilde{E}_t \end{bmatrix}}_{\text{nonlinear disturbance}},$$

Nonlinear Disturbance Flow Formulation: NLDE

$$\frac{\partial \mathbf{W}}{\partial t} + \frac{\partial \mathbf{F}}{\partial x} + \frac{\partial \mathbf{G}}{\partial y} + \frac{\partial \mathbf{H}}{\partial z} = 0,$$

3D Compressible N.S. in vector form

$$\mathbf{W} = \bar{\mathbf{W}} + \tilde{\mathbf{W}} = \bar{\mathbf{W}} + \tilde{\mathbf{W}}_l + \tilde{\mathbf{W}}_{nl} = \underbrace{\begin{bmatrix} \bar{\rho} \\ \bar{\rho}\bar{u} \\ \bar{\rho}\bar{v} \\ \bar{\rho}\bar{w} \\ \bar{\rho}\bar{E}_t \end{bmatrix}}_{\text{baseflow}} + \underbrace{\begin{bmatrix} \tilde{\rho} \\ \tilde{\rho}\bar{u} + \bar{\rho}\tilde{u} \\ \tilde{\rho}\bar{v} + \bar{\rho}\tilde{v} \\ \tilde{\rho}\bar{w} + \bar{\rho}\tilde{w} \\ \tilde{\rho}\bar{E}_t + \tilde{\rho}\bar{E}_t \end{bmatrix}}_{\text{linear disturbance}} + \underbrace{\begin{bmatrix} \\ \tilde{\rho}\tilde{u} \\ \tilde{\rho}\tilde{v} \\ \tilde{\rho}\tilde{w} \\ \tilde{\rho}\tilde{E}_t \end{bmatrix}}_{\text{nonlinear disturbance}},$$

Viscous flux

$$\mathbf{F_v} = -\underbrace{\begin{bmatrix} 0 \\ \bar{\mu}\bar{\tau}_{xx} \\ \bar{\mu}\bar{\tau}_{xy} \\ \bar{\mu}\bar{\tau}_{xz} \\ \bar{\mathcal{E}} \end{bmatrix}}_{\text{baseflow}} - \underbrace{\begin{bmatrix} 0 \\ \bar{\mu}\tilde{\tau}_{xx} + \tilde{\mu}\bar{\tau}_{xx} \\ \bar{\mu}\tilde{\tau}_{xy} + \tilde{\mu}\bar{\tau}_{xy} \\ \bar{\mu}\tilde{\tau}_{xz} + \tilde{\mu}\bar{\tau}_{xz} \\ \tilde{\mathcal{E}}_l \end{bmatrix}}_{\text{linear disturbance}} - \underbrace{\begin{bmatrix} 0 \\ \tilde{\mu}\tilde{\tau}_{xx} \\ \tilde{\mu}\tilde{\tau}_{xy} \\ \tilde{\mu}\tilde{\tau}_{xz} \\ \tilde{\mathcal{E}}_{nl} \end{bmatrix}}_{\text{nonlinear disturbance}},$$

$$\mathbf{F_c} = \underbrace{\begin{bmatrix} \bar{\rho}\bar{u} \\ \bar{\rho}\bar{u}^2 + \bar{p} \\ \bar{\rho}\bar{u}\bar{v} \\ \bar{\rho}\bar{u}\bar{w} \\ (\bar{\rho}\bar{E}_t + \bar{p})\bar{u} \end{bmatrix}}_{\text{baseflow}} + \underbrace{\begin{bmatrix} \tilde{\rho}\bar{u} + \bar{\rho}\tilde{u} \\ \tilde{\rho}\bar{u}^2 + 2\bar{\rho}\bar{u}\tilde{u} + \tilde{p} \\ \tilde{\rho}\bar{u}\bar{v} + \bar{\rho}\bar{u}\tilde{v} + \bar{\rho}\tilde{u}\bar{v} \\ \tilde{\rho}\bar{u}\bar{w} + \bar{\rho}\bar{u}\tilde{w} + \bar{\rho}\tilde{u}\bar{w} \\ (\tilde{\rho}\bar{E}_t + \bar{\rho}\tilde{E}_t + \tilde{p})\bar{u} + (\bar{\rho}\bar{E}_t + \bar{p})\tilde{u} \end{bmatrix}}_{\text{linear disturbance}} + \underbrace{\begin{bmatrix} \tilde{\rho}\tilde{u} \\ \bar{\rho}\tilde{u}^2 + \tilde{\rho}\tilde{u}^2 + 2\tilde{\rho}\bar{u}\tilde{u} \\ \tilde{\rho}\bar{u}\tilde{v} + \tilde{\rho}\tilde{u}\bar{v} + \bar{\rho}\tilde{u}\tilde{v} + \tilde{\rho}\tilde{u}\tilde{v} \\ \tilde{\rho}\bar{u}\tilde{w} + \tilde{\rho}\tilde{u}\bar{w} + \bar{\rho}\tilde{u}\tilde{w} + \tilde{\rho}\tilde{u}\tilde{w} \\ (\tilde{\rho}\bar{E}_t + \bar{\rho}\tilde{E}_t + \tilde{\rho}\tilde{E}_t + \tilde{p})\tilde{u} + \tilde{\rho}\tilde{E}_t\bar{u} \end{bmatrix}}_{\text{nonlinear disturbance}},$$

Convective flux

$$\begin{aligned}
\bar{\mathcal{E}} &= -\bar{\mu}\left(\bar{u}\bar{\tau}_{xx} + \bar{v}\bar{\tau}_{xy} + \bar{w}\bar{\tau}_{xz}\right) - \bar{k}\frac{\partial \bar{T}}{\partial x}, \\
\tilde{\mathcal{E}}_l &= -\bar{\mu}\left(\bar{u}\tilde{\tau}_{xx} + \tilde{u}\bar{\tau}_{xx} + \bar{v}\tilde{\tau}_{xy} + \tilde{v}\bar{\tau}_{xy} + \bar{w}\tilde{\tau}_{xz} + \tilde{w}\bar{\tau}_{xz}\right) - \\
&\quad \tilde{\mu}\left(\bar{u}\bar{\tau}_{xx} + \bar{v}\bar{\tau}_{xy} + \bar{w}\bar{\tau}_{xz}\right) - \bar{k}\frac{\partial \tilde{T}}{\partial x} - \tilde{k}\frac{\partial \bar{T}}{\partial x}, \quad \text{and} \\
\tilde{\mathcal{E}}_{nl} &= -\bar{\mu}\left(\tilde{u}\tilde{\tau}_{xx} + \tilde{v}\tilde{\tau}_{xy} + \tilde{w}\tilde{\tau}_{xz}\right) - \\
&\quad \tilde{\mu}\left(\tilde{u}\tilde{\tau}_{xx} + \tilde{u}\bar{\tau}_{xx} + \tilde{u}\tilde{\tau}_{xx} + \tilde{v}\tilde{\tau}_{xy} + \tilde{v}\bar{\tau}_{xy} + \tilde{v}\tilde{\tau}_{xy} + \tilde{w}\tilde{\tau}_{xz} + \tilde{w}\bar{\tau}_{xz} + \tilde{w}\tilde{\tau}_{xz}\right) - \tilde{k}\frac{\partial \tilde{T}}{\partial x}.
\end{aligned}$$

Nonlinear Disturbance Flow Formulation: NLDE

$$\frac{\partial \mathbf{W}}{\partial t} + \frac{\partial \mathbf{F}}{\partial x} + \frac{\partial \mathbf{G}}{\partial y} + \frac{\partial \mathbf{H}}{\partial z} = 0,$$

3D Compressible N.S. eqns in vector form

$$\mathbf{W} = \bar{\mathbf{W}} + \tilde{\mathbf{W}} = \bar{\mathbf{W}} + \tilde{\mathbf{W}}_l + \tilde{\mathbf{W}}_{nl} = \underbrace{\begin{bmatrix} \bar{\rho} \\ \bar{\rho}\bar{u} \\ \bar{\rho}\bar{v} \\ \bar{\rho}\bar{w} \\ \bar{\rho}\bar{E}_t \end{bmatrix}}_{\text{baseflow}} + \underbrace{\begin{bmatrix} \tilde{\rho} \\ \tilde{\rho}\bar{u} + \bar{\rho}\tilde{u} \\ \tilde{\rho}\bar{v} + \bar{\rho}\tilde{v} \\ \tilde{\rho}\bar{w} + \bar{\rho}\tilde{w} \\ \bar{\rho}\tilde{E}_t + \tilde{\rho}\bar{E}_t \end{bmatrix}}_{\text{linear disturbance}} + \underbrace{\begin{bmatrix} \\ \tilde{\rho}\tilde{u} \\ \tilde{\rho}\tilde{v} \\ \tilde{\rho}\tilde{w} \\ \tilde{\rho}\tilde{E}_t \end{bmatrix}}_{\text{nonlinear disturbance}},$$

$$\frac{\partial \tilde{\mathbf{W}}}{\partial t} + \frac{\partial \tilde{\mathbf{F}}}{\partial x} + \frac{\partial \tilde{\mathbf{G}}}{\partial y} + \frac{\partial \tilde{\mathbf{H}}}{\partial z} = -\left(\frac{\partial \bar{\mathbf{W}}}{\partial t} + \frac{\partial \bar{\mathbf{F}}}{\partial x} + \frac{\partial \bar{\mathbf{G}}}{\partial y} + \frac{\partial \bar{\mathbf{H}}}{\partial z} \right).$$

$$\frac{\partial \tilde{\mathbf{W}}}{\partial t} + \frac{\partial \tilde{\mathbf{F}}}{\partial x} + \frac{\partial \tilde{\mathbf{G}}}{\partial y} + \frac{\partial \tilde{\mathbf{H}}}{\partial z} = 0.$$

3D Compressible N.S. disturbance flow eqns

AMR Dual-Mesh Approach

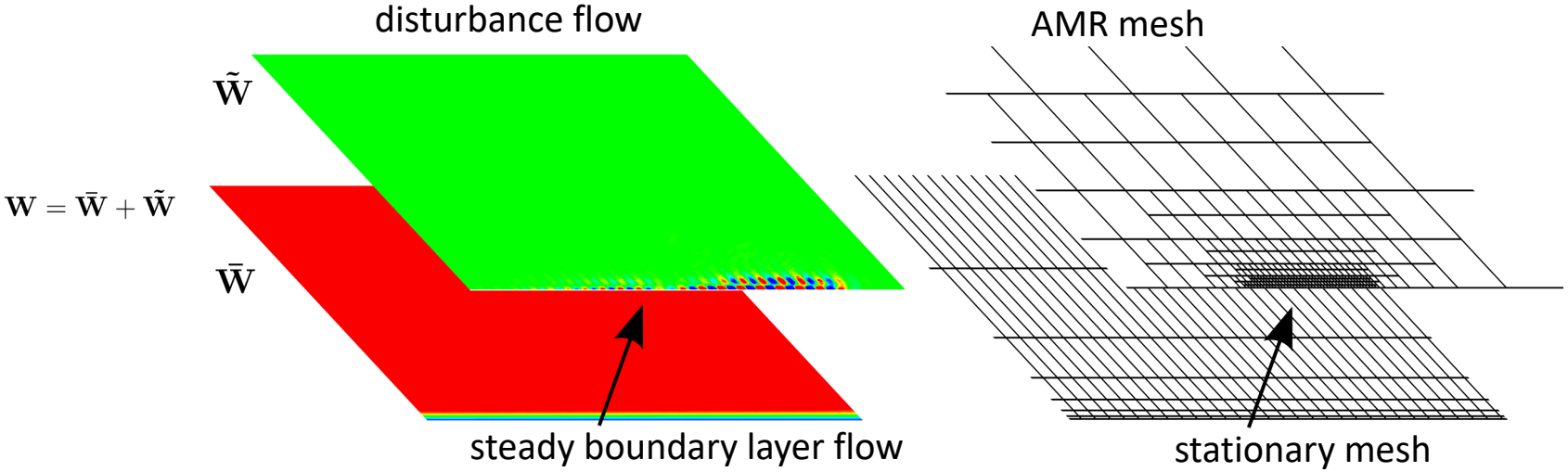

- **AMR is a proven methodology for multi-scale problems** with an extensive existing mathematical and software knowledge base
- **Higher-order accurate inter-level operators** (implementation is similar to Kiris *et al*. (2018))
- Octree-based donor cell search algorithm for **dual-mesh approach**
- **Sensitivity parameter φ** controls mesh refinement/derefinement

  $\varphi = max\left(\frac{|\phi_1'|}{max(|\phi_1'|)}, \frac{|\phi_2'|}{max(|\phi_2'|)}, \ldots.\right)$ based on tracking variable $\phi'(\boldsymbol{x}, t, \boldsymbol{Q}')$
- What is the best set of tracking variables? **Compromise between efficiency vs. accuracy!**

AMR Dual-Mesh Approach

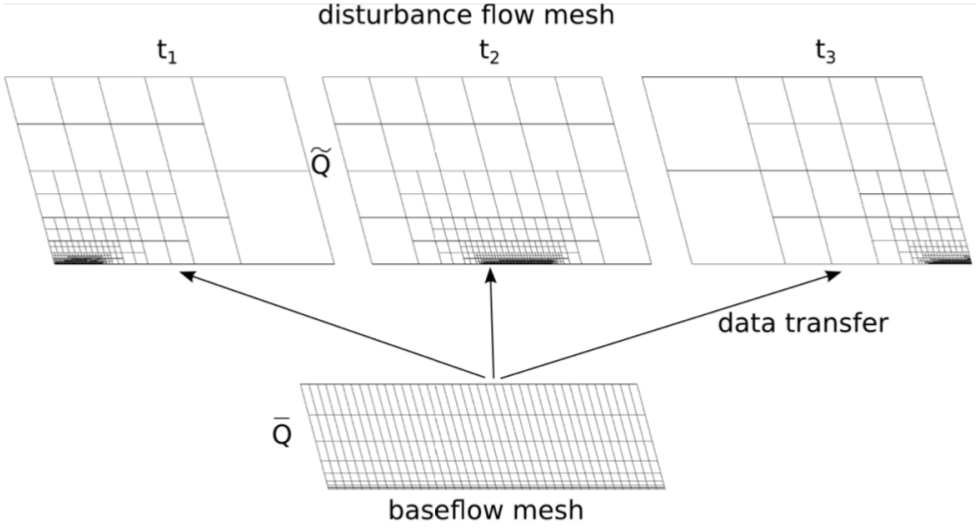

Disturbance flow formulation of 3D compressible Navier-Stokes Equations

$$\frac{\partial \tilde{\mathbf{W}}}{\partial t} + \frac{\partial \tilde{\mathbf{E}}}{\partial x} + \frac{\partial \tilde{\mathbf{F}}}{\partial y} + \frac{\partial \tilde{\mathbf{G}}}{\partial z} = 0.$$

High grid resolution is only required locally, and temporal sub-cycling on the octree-based block-structured Cartesian mesh allows to efficiently simulate particles over time.

Validation case: M=5.35 Flat Plate Boundary Layer, strongly nonlinear amplitude pulse

O. M. F. Browne, A. P. Haas, H. F. Fasel, and C. Brehm. An efficient strategy for computing wave-packets in high-speed boundary layers. In 47th AIAA Fluid Dynamics Conference, Denver, CO, 2017.

O. M. F. Browne, A. P. Haas, H. F. Fasel, and C. Brehm. An efficient linear wavepacket tracking method for hypersonic boundary-layer stability prediction. J. Comput. Phys., 380:243–268, 2019.

A. P. Haas, O. M. F. Browne, H. F. Fasel, and C. Brehm. A numerical jacobian stability-solver based on the linearized compressible navier-stokes equations. In 47th AIAA Fluid Dynamics Conference, Denver, CO, 2017.

O. M. F. Browne, A. P. Haas, H. F. Fasel, and C. Brehm. An efficient nonlinear wavepacket tracking method for hypersonic boundary-layer flows. JCP, revised.

A. P. Haas, O. M. F. Browne, H. F. Fasel, and C. Brehm. A time-spectral numerical jacobian based linearized compressible navier-stokes solver for hypersonic boundary-layer stability. JCP, accepted.

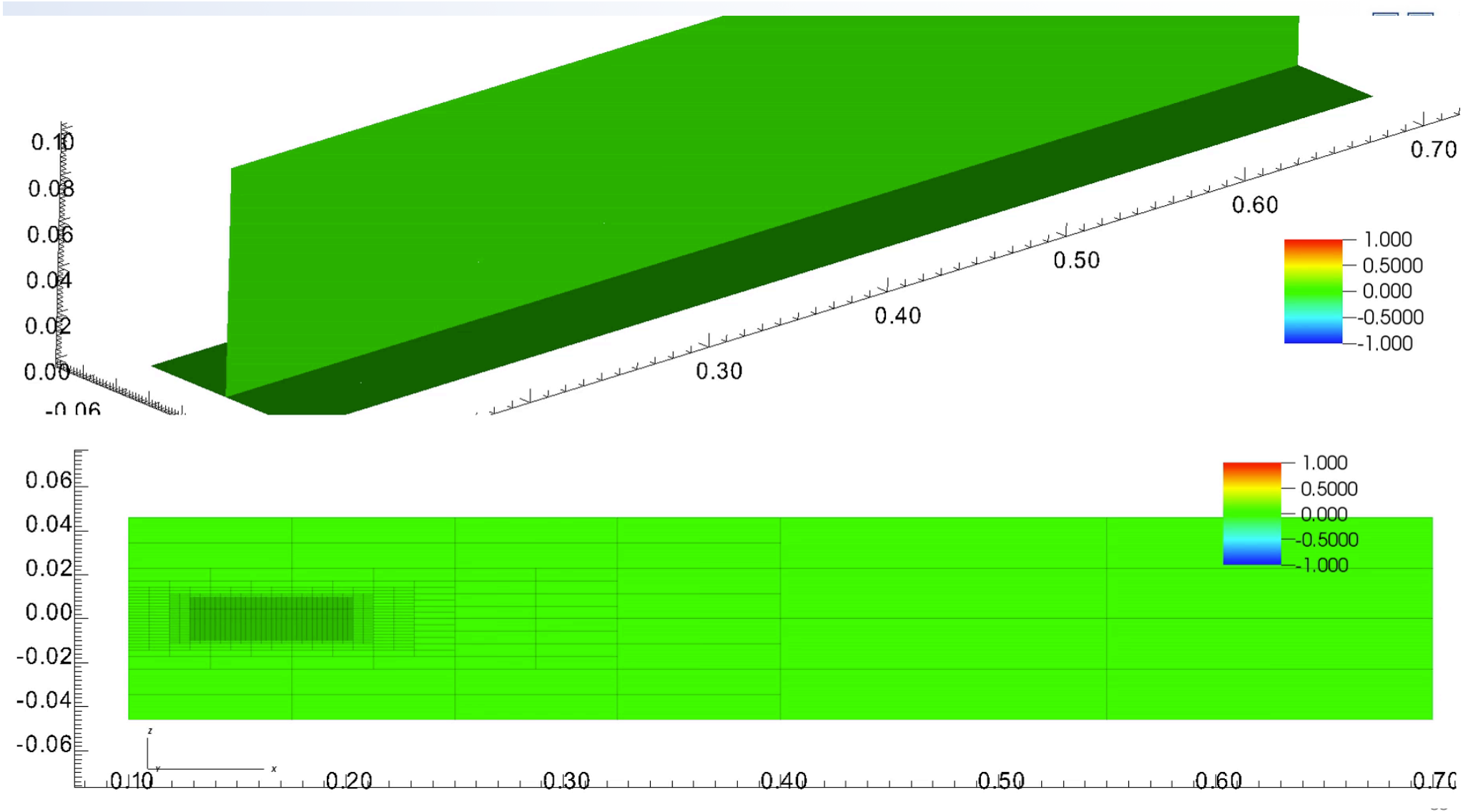
0.10
0.08
0.06
0.04
0.02
0.00
0.30
0.40
0.50
0.60
0.70
1.000
0.5000
0.000
-0.5000
-1.000
0.06
0.04
0.02
0.00
-0.02
-0.04
-0.06
0.10
0.20
0.30
0.40
0.50
0.60
0.70
1.000
0.5000
0.000
-0.5000
-1.000

Comparison Against Standard DNS Approach

Current AMR Approach

Sivasubramanian et al. 2011

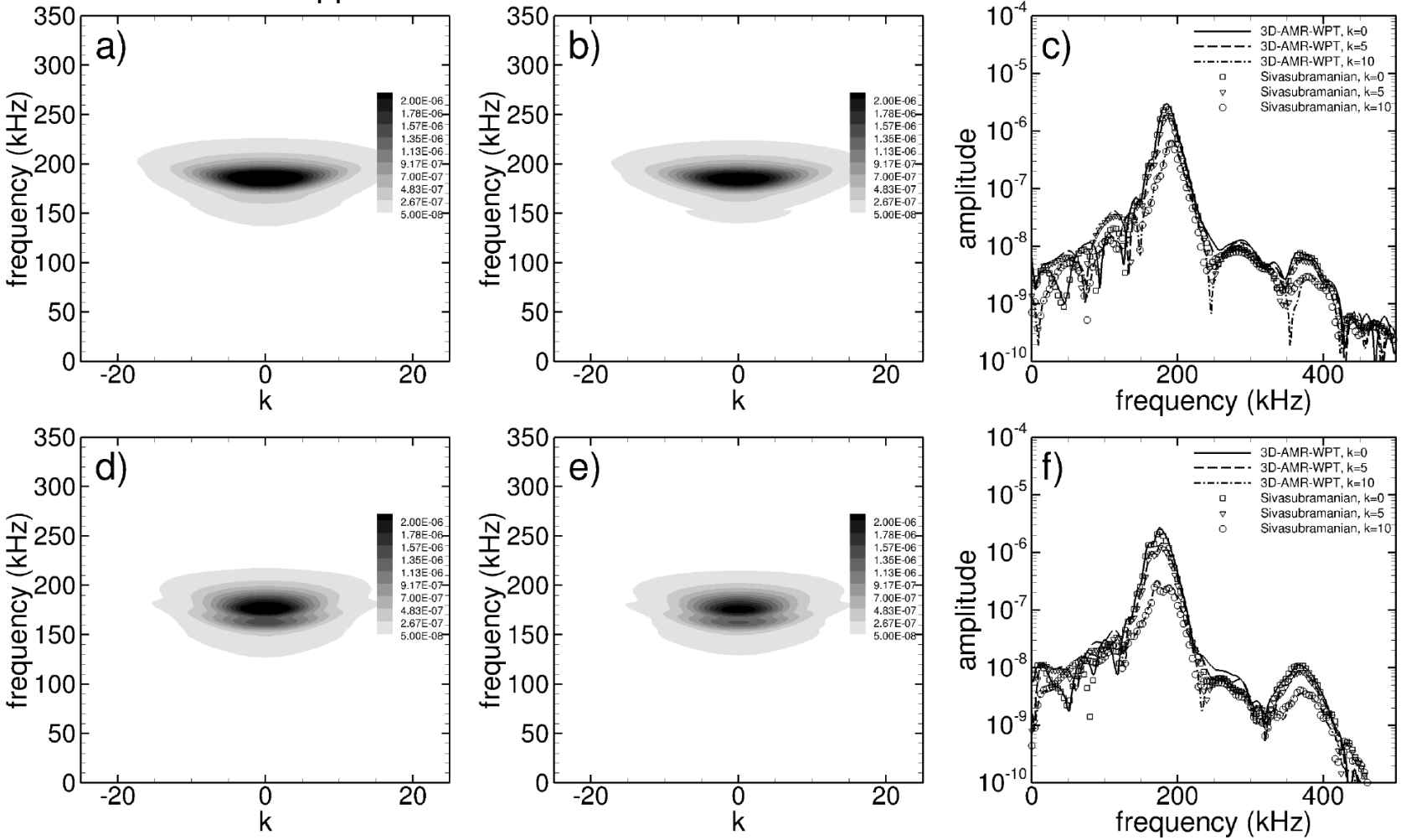

Comparison Against Standard DNS Approach

Current AMR Approach

Sivasubramanian et al. 2011

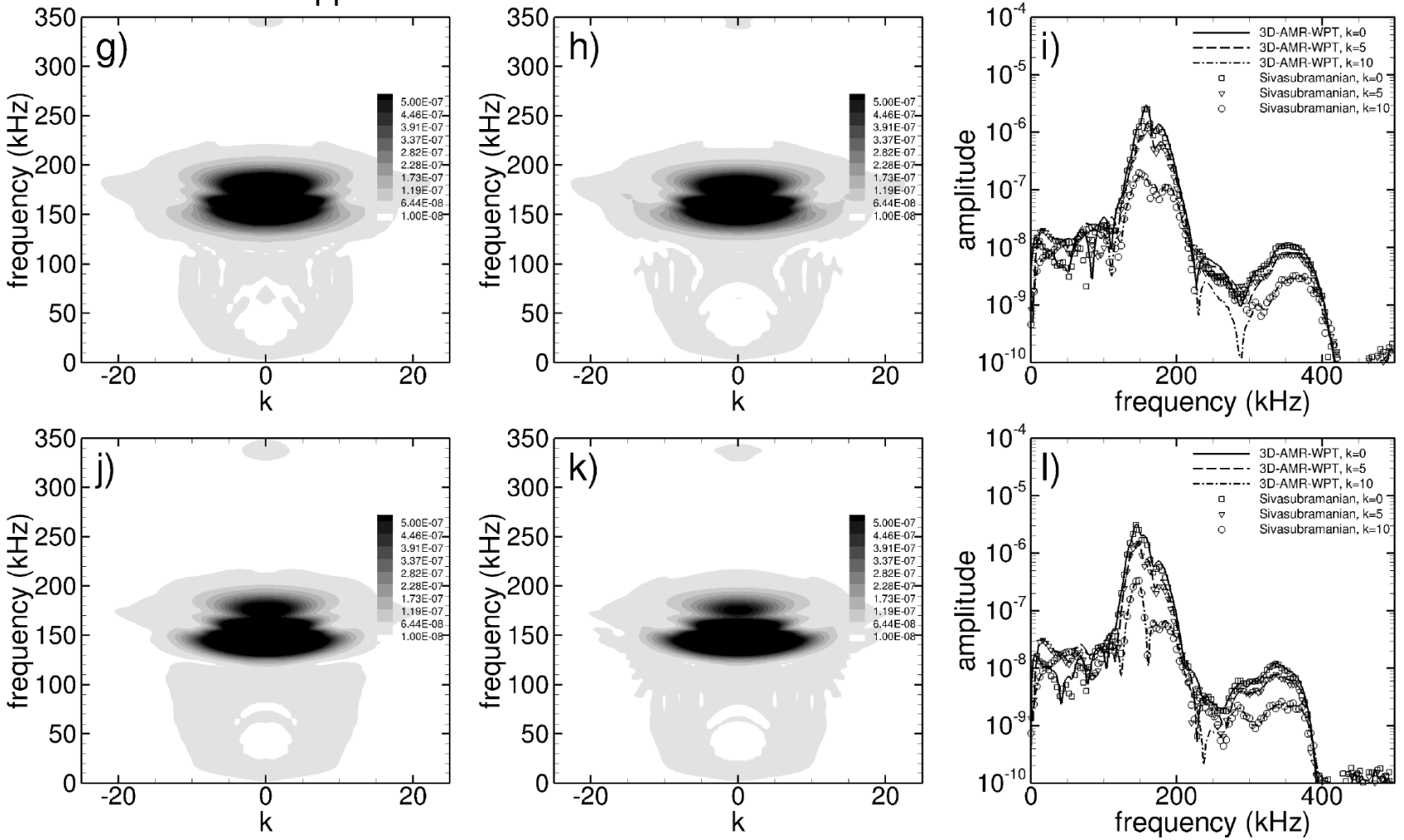

Comparison Against Standard DNS Approach

Current AMR Approach

Sivasubramanian et al. 2011

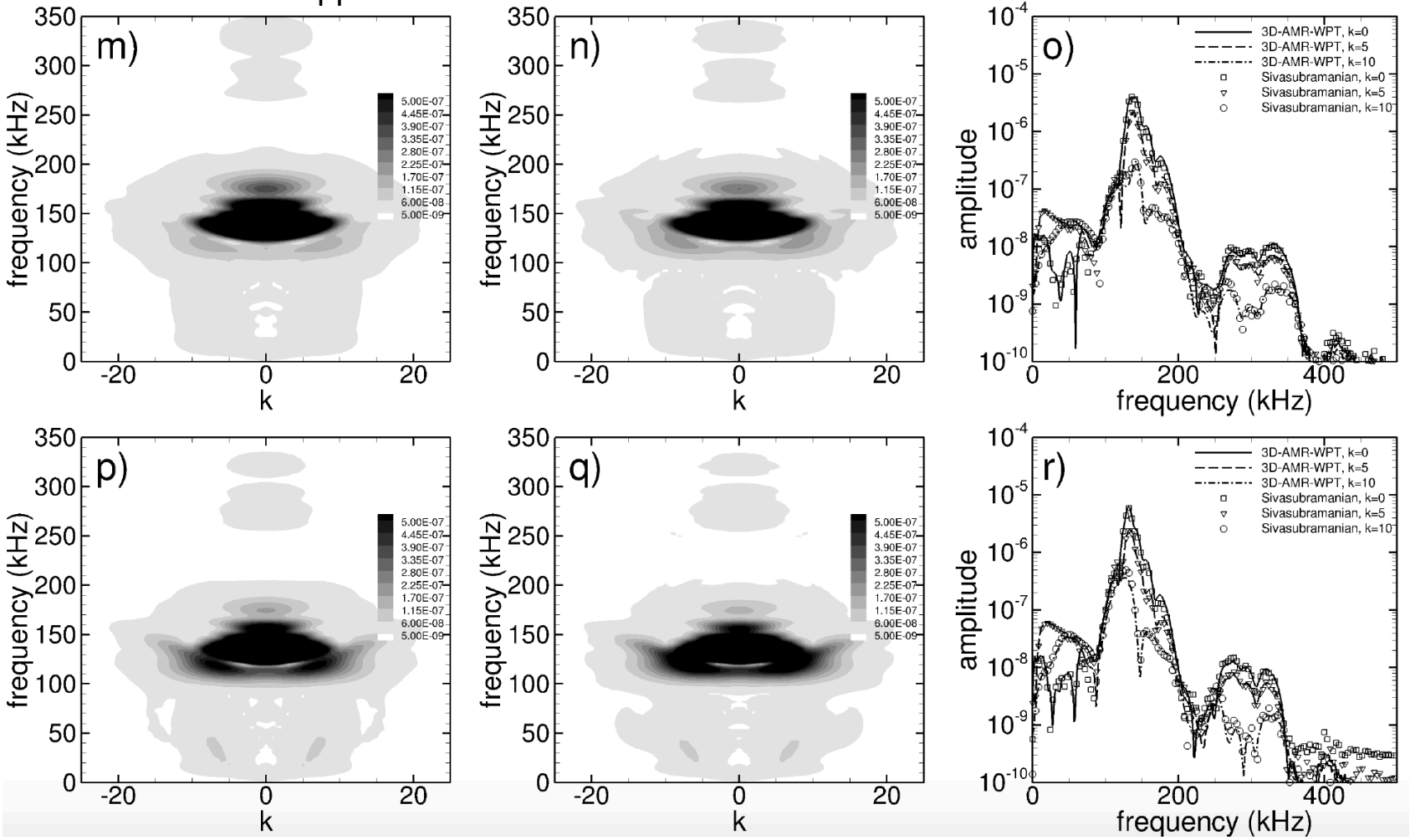

Particle Model

Particle-Source-In-Cell Method Simulation Approach

Kinematic equations:

$$\frac{d\mathbf{x}_p}{dt} = \mathbf{v}_p,$$

Newton's second law:

$$m_p \frac{d\mathbf{v}_p}{dt} = \mathbf{F}_p,$$

Force by Chuvakhov et al. (2019):

$$\mathbf{F}_p = -\frac{1}{2} C_D \rho \left|\mathbf{v}_p - \mathbf{v}\right| \left(\mathbf{v}_p - \mathbf{v}\right) \pi R_p^2.$$

$\mathbf{x_p}$ = particle position

$\mathbf{v_p}$ = particle velocity

C_D = drag coefficient

R_p = particle radius

v = fluid velocity

ρ = fluid density

Re = relative Reynolds number

M = relative Mach number

Crowe (1967)

$$C_D = \left(C_{D,in} - 2\right) e^{\left(-3.632\left(\frac{M}{Re} g(Re)\right)\right)} + \frac{h\left(M\right)}{1.183M} e^{\left(-\frac{Re}{2M}\right)} + 2,$$

$$\log_{10}\left(g\left(Re\right)\right) = 1.25\left(1 + \tanh\left(0.77\log_{10}\left(Re\right) - 1.92\right)\right), \quad \text{and}$$

$$h(M) = 2.3 + 1.7\left(\frac{T_p}{T}\right)^{0.5} - 2.3\tanh\left(1.17\log_{10}\left(M\right)\right).$$

Morrison (2013):

$$C_{D,in} = \frac{24}{Re} + \frac{2.6\left(\frac{Re}{5}\right)}{1 + \left(\frac{Re}{5}\right)^{1.52}} + \frac{0.411\left(\frac{Re}{2.63\times10^5}\right)^{-7.94}}{1 + \left(\frac{Re}{2.63\times10^5}\right)^{-8}} + \frac{0.25\left(\frac{Re}{10^6}\right)}{1 + \left(\frac{Re}{10^6}\right)},$$

Different Positions

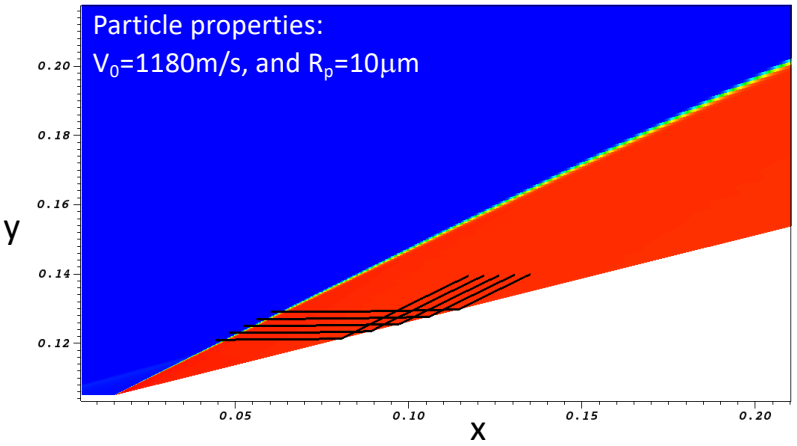

Different Values of Collision Coefficient

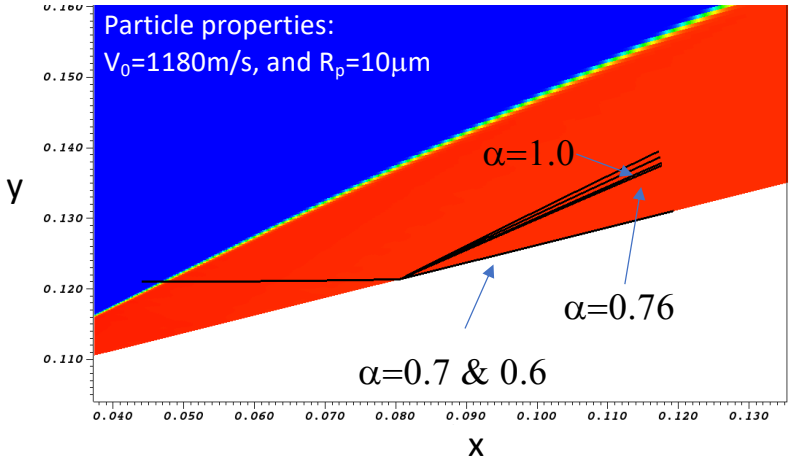

Elastic vs. Inelastic Collision

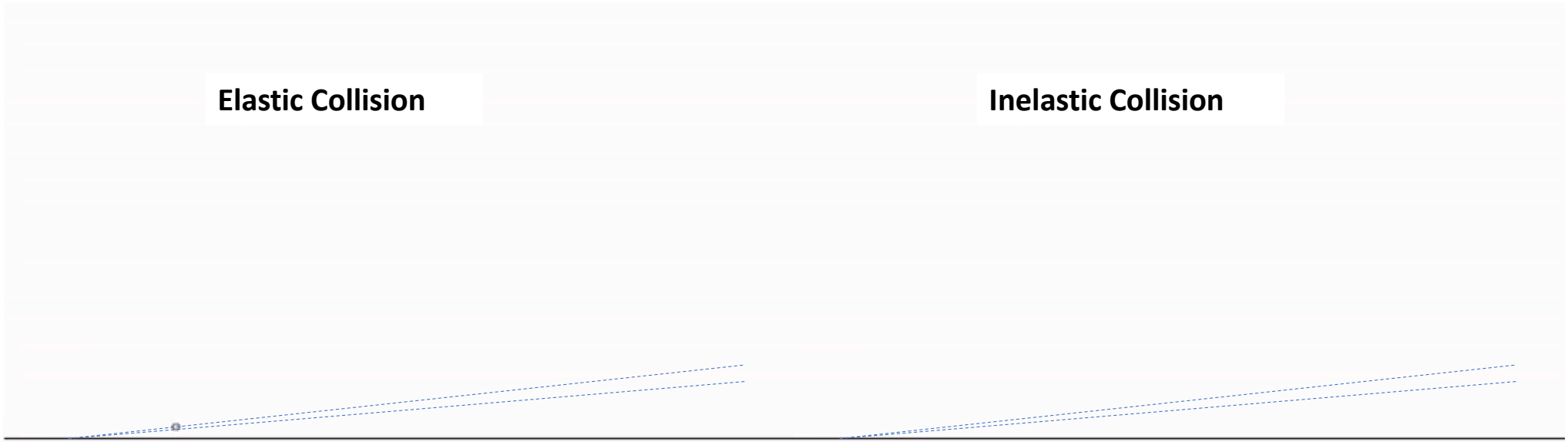

Note: Dashed lines mark approximate path of particle.

Outline

Particle Flow Simulations Background

Background, prior research and findings.

Numerical Methods

BitCart, Dual-Mesh Approach, and AMR.

Simulations Results

Validation, and 2D/3D patricle flow simulations results.

Summary, Outlook, & Research Interest

Summary of presented research

DNS of Particle Impingement for Mach 6 Flow

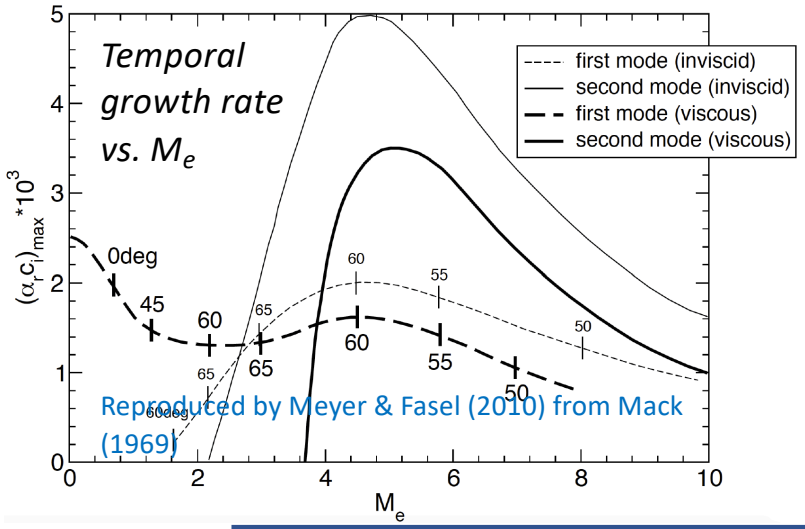

Reproduced by Meyer & Fasel (2010) from Mack (1969)

- Two-Step Simulation Approach:
  1.) baseflow computation & 2.) AMR particle tracking simulation
- Particle flow simulation approach was initially tested in 2-D (or axisymmetric) flows
- Initial 2-D simulations involve flows where second mode is the most dominant instability mechanism

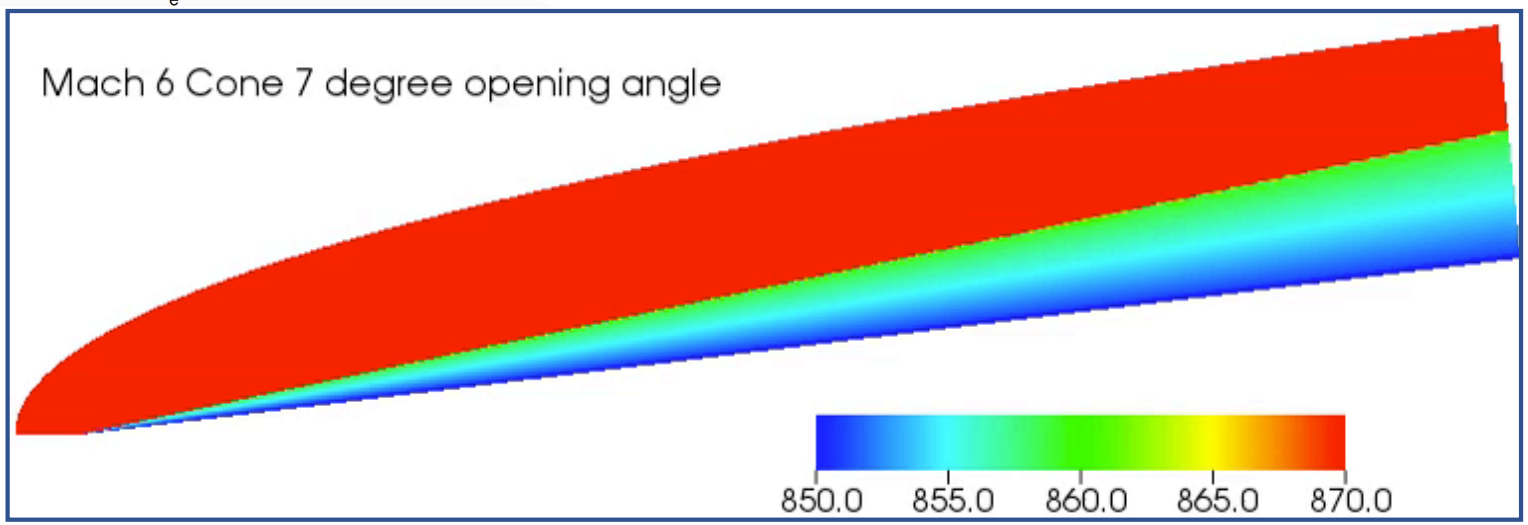

Pressure Signature

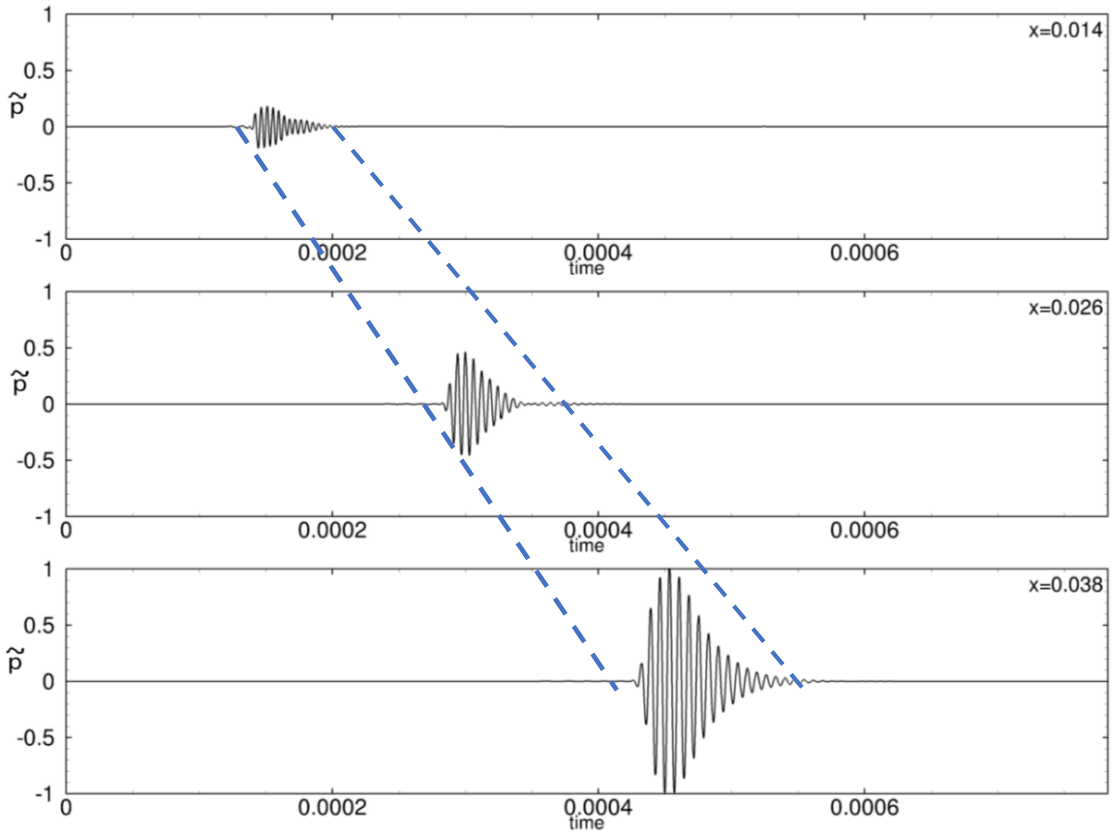

- Disturbance pressure signal is sampled at the wall via point probes,
- After performing an FFT on the signals, the dominant and amplified wavenumbers/frequencies can be obtained,
- The type of instability (first, second, higher-modes, cross-flow etc) that is introduced can be identified,
- Calculating N-factors can be used to predict transition location,
- Moving towards biorthogonal decomposition with Tumin (UofA).

Flow Visualization – Disturbance Pressure

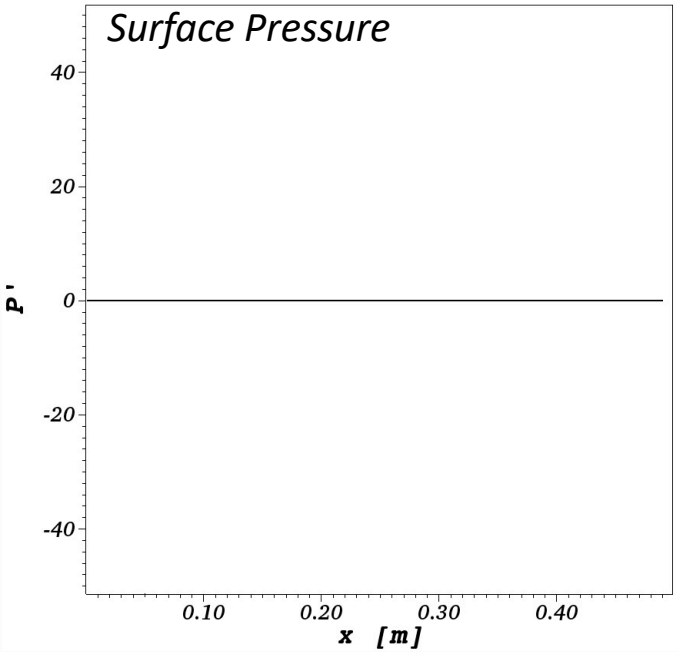

- Mach 5.35 Boundary Layer Flow
  After shock conditions:
  p_∞=1297 Pa, ρ_∞=0.071 kg/m^3,
  T_∞=63.9 K & Re=14.6·10^{6}m^{-1}

- Particle properties:
  ρ_p=1000 kg/m^3, R_p=5 μm
  $\mathbf{V_p}$=[cos(7°),sin(7°)] 871 m/s
  $\mathbf{x_p}$=[0.11,0.004] m & Re_p≈146

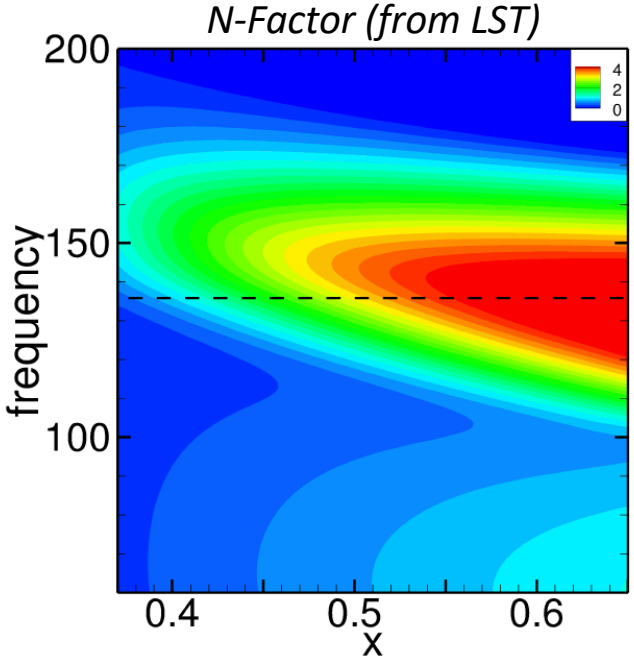

Contours of Disturbance Pressure

Pressure Signature

Particle collision location located upstream of neutral curve

Pulse Disturbance – trigger second mode

Particle Simulations

Linear

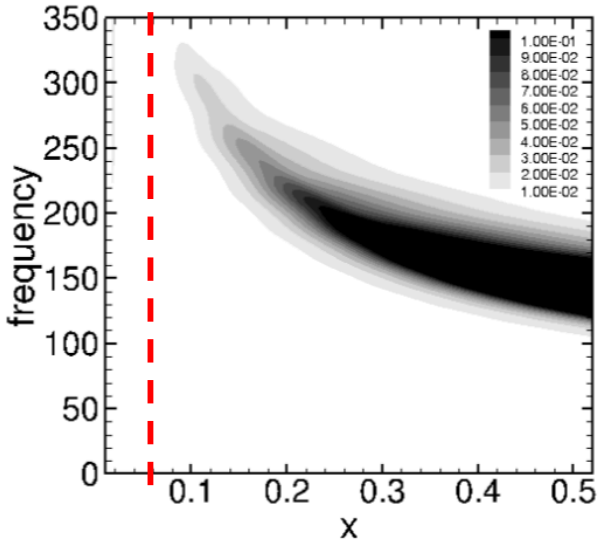

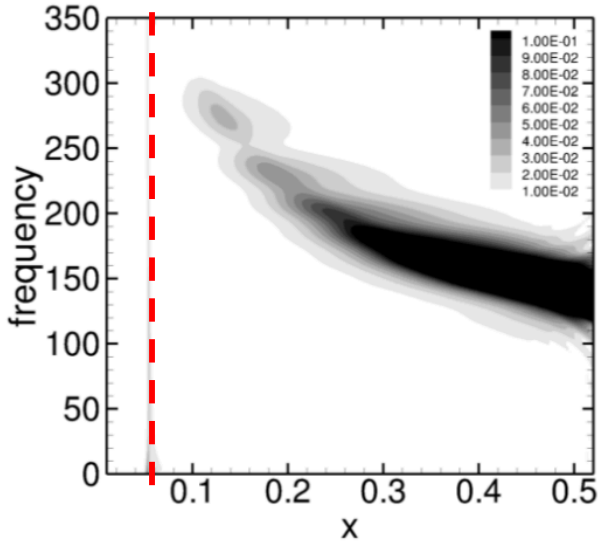

Nonlinear

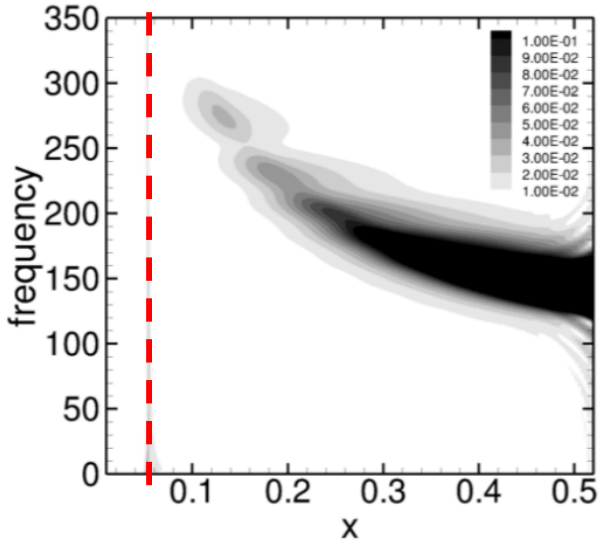

- Particles of size 10μm leads to non-dimensional pressure signature of $p_0'/p_\infty = \mathcal{O}(10^{-3} - 10^{-4})$
- Pressure signature is highly dependent on flow conditions, particle properties, impingement location, etc.

Pressure Signature

Particle collision location located upstream of neutral curve

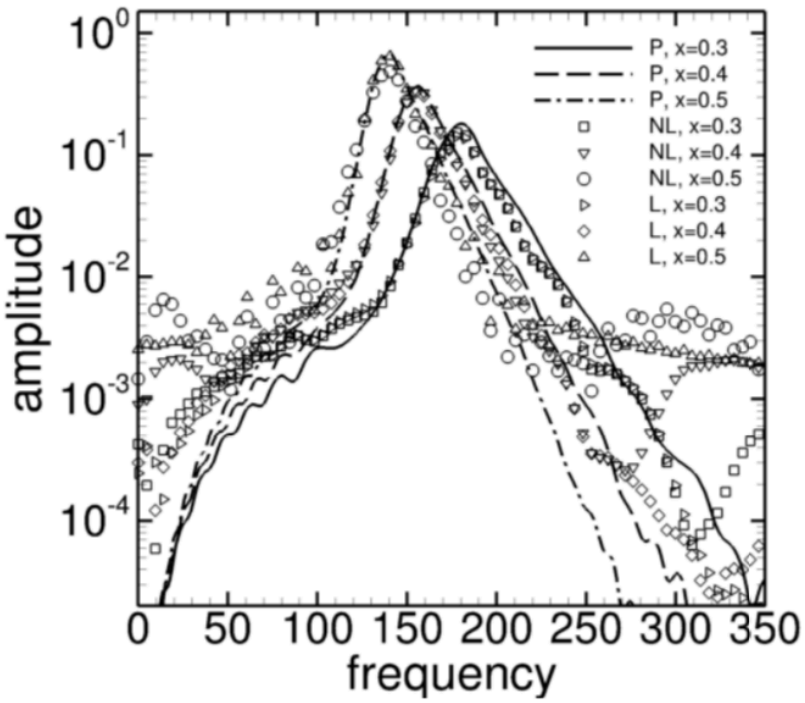

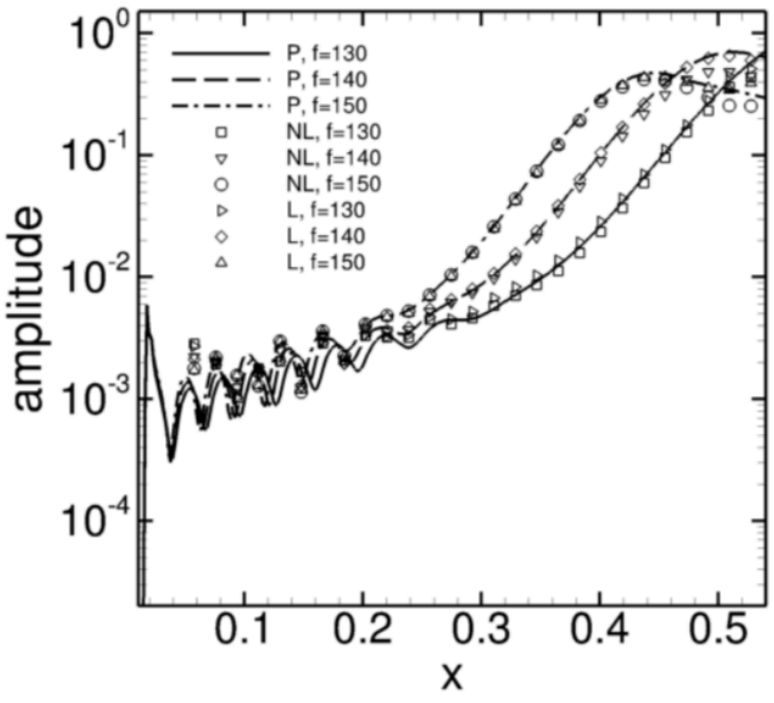

- Particles of size 10μm leads to non-dimensional pressure signature of $p_0'/p_\infty = \mathcal{O}(10^{-3} - 10^{-4})$
- Pressure signature is highly dependent on flow conditions, particle properties, impingement location, etc.

Pressure Signature

Particle collision location located upstream of neutral curve

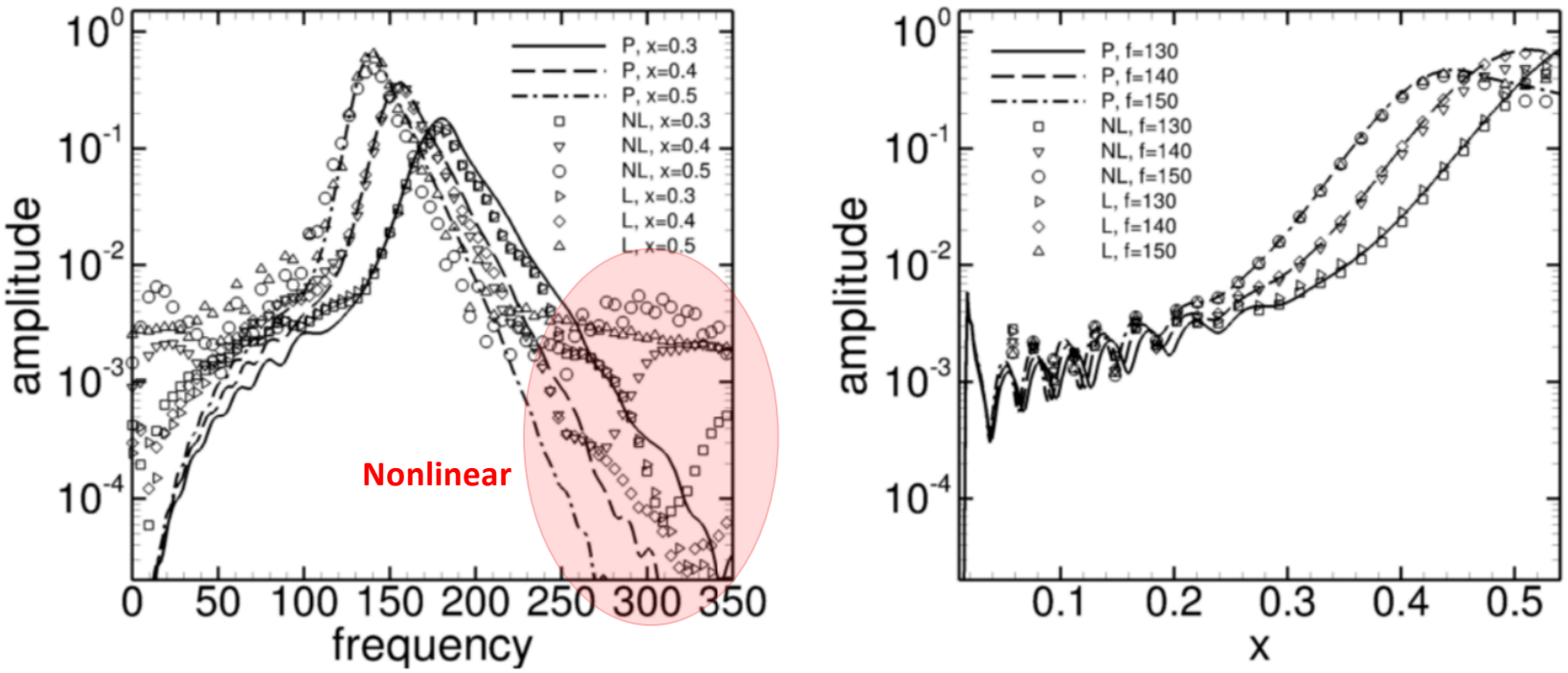

- Particles of size 10μm leads to non-dimensional pressure signature of $p_0'/p_\infty = \mathcal{O}(10^{-3} - 10^{-4})$
- Pressure signature is highly dependent on flow conditions, particle properties, impingement location, etc.

Pressure Signature

Particle collision location located downstream of neutral curve

Pulse Disturbance

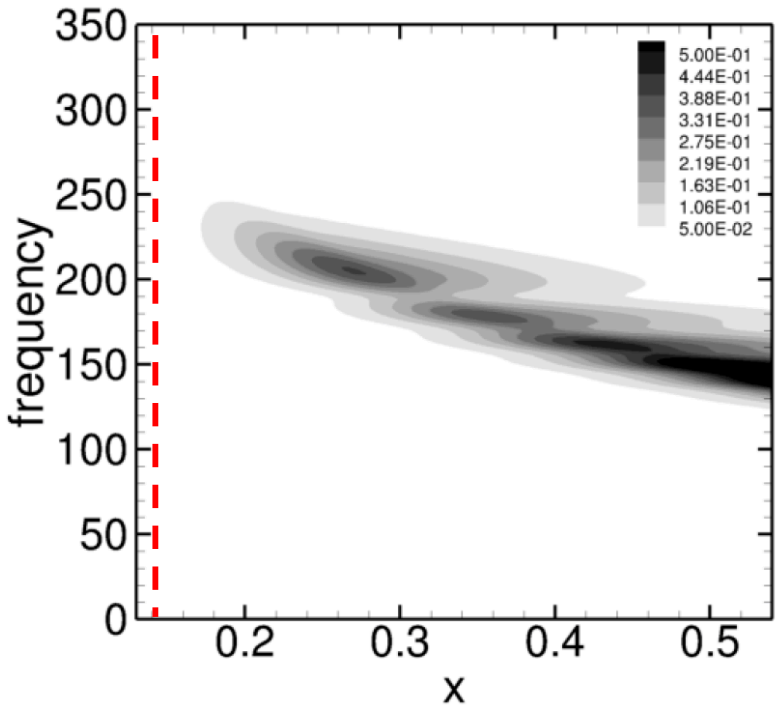

Particle Simulations

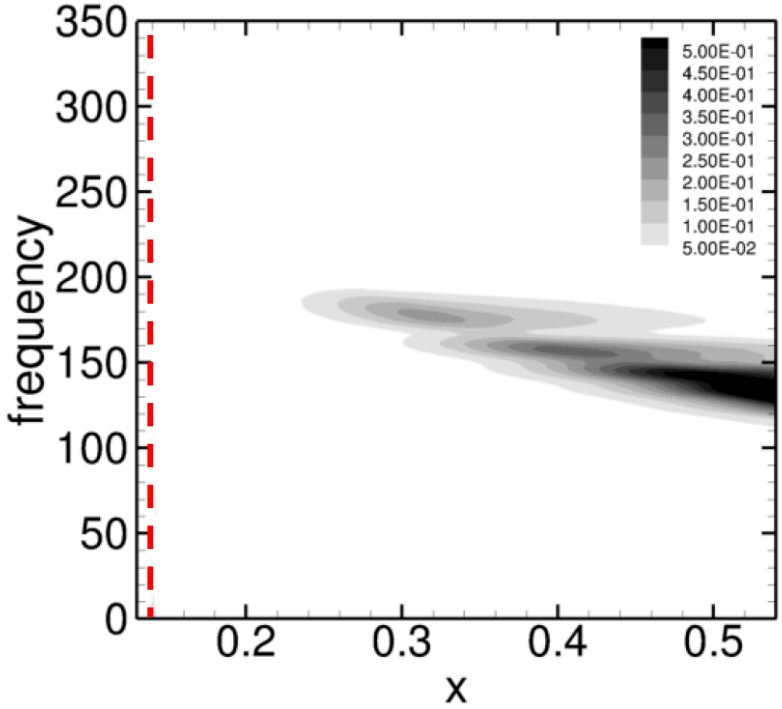

- Particle impingement at downstream location inside neutral curve for relevant frequencies
- Results for pulse and particle simulations are very different (due to initial disturbance level and receptivity)

Pressure Signature

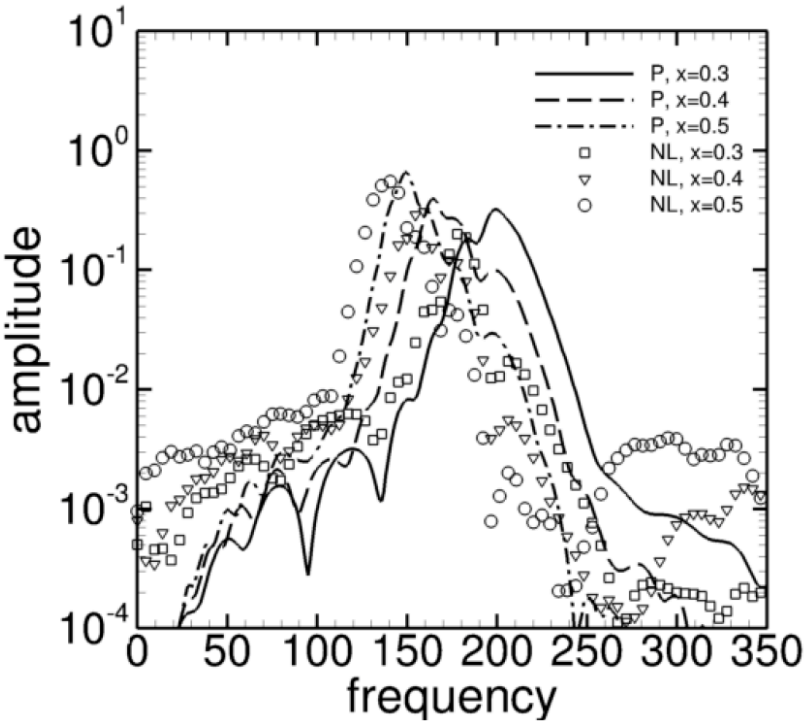

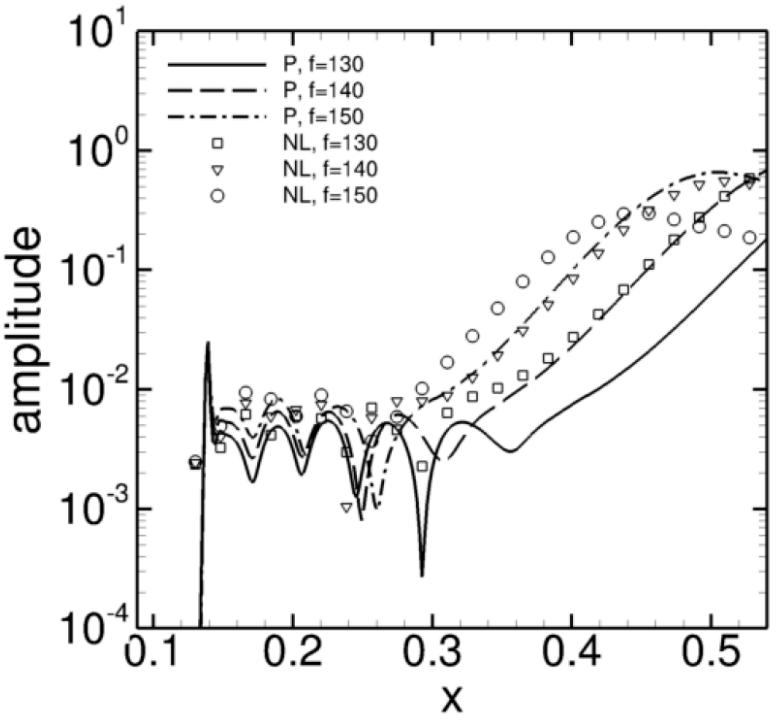

- Particle impingement at downstream location inside neutral curve for relevant frequencies
- Results for pulse and particle simulations are very different (due to initial disturbance level and receptivity)

Effects of Particle Size

Particle with D_p=10μm

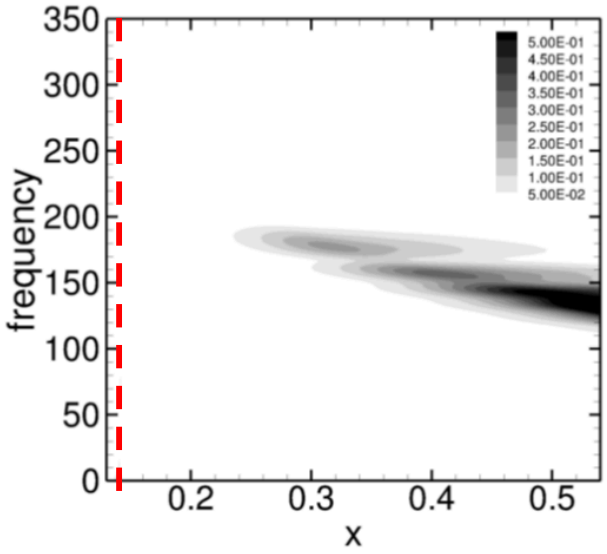

Particle with D_p=50μm

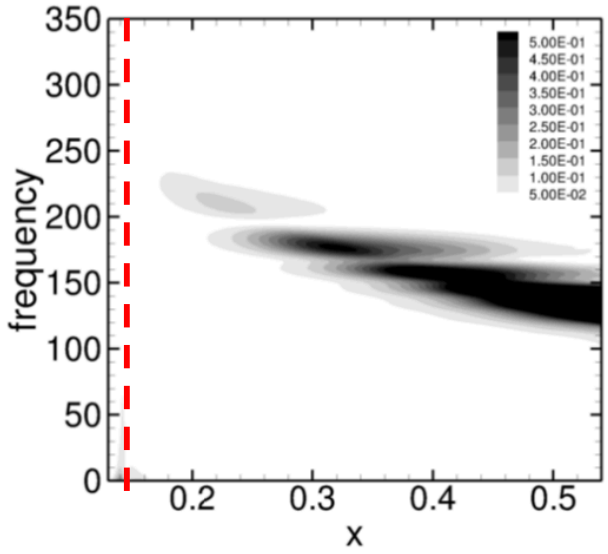

Particle with D_p=100μm

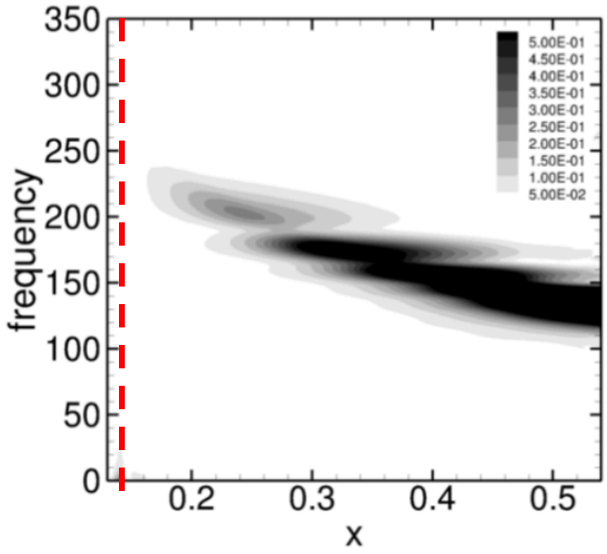

- Broad frequency spectrum introduced by particle collision (with low frequency peak)
- Particle collision location downstream of neutral curve,

Effects of Particle Size

Pressure amplitude versus frequency for different particle sizes

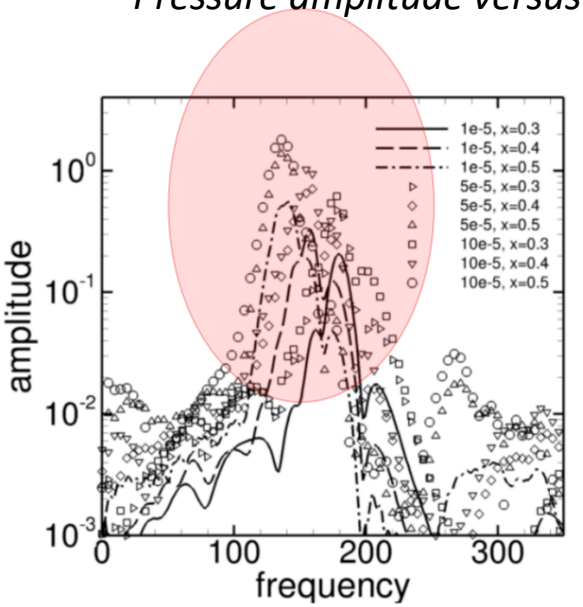

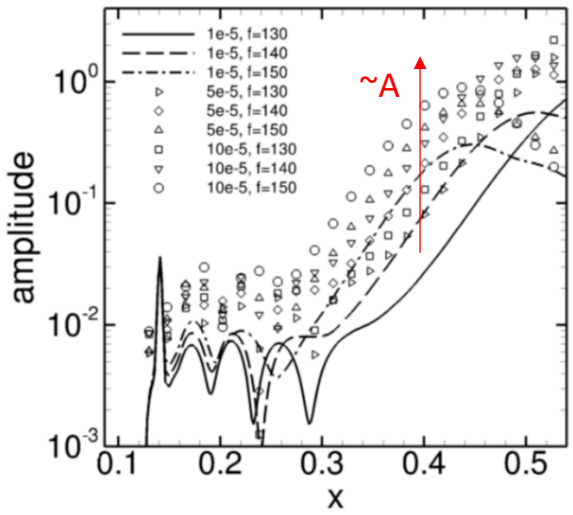

Fedorov (2013)

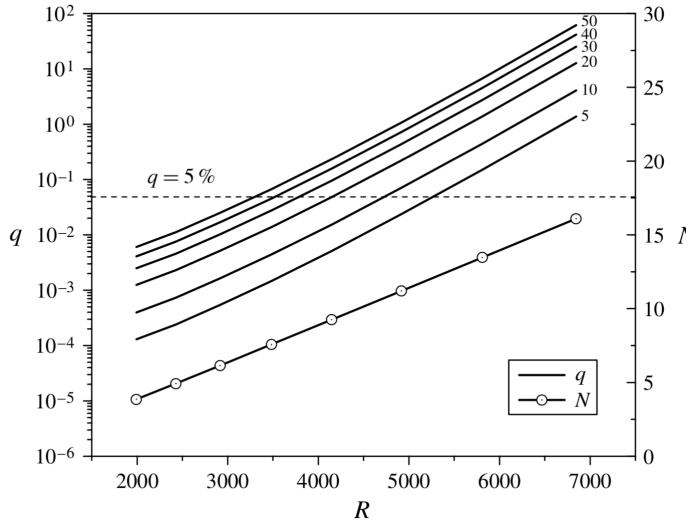

- As expected, larger particle size lead to vertical shift in amplitude curves
- In addition to higher disturbance amplitudes, a change in spectrum is observed
- Rough estimate for excitation frequency captures first peak in the spectrum ($f \sim v_p/2\delta_{99}$),

Effects of Particle Size

Pressure amplitude versus frequency for different particle sizes

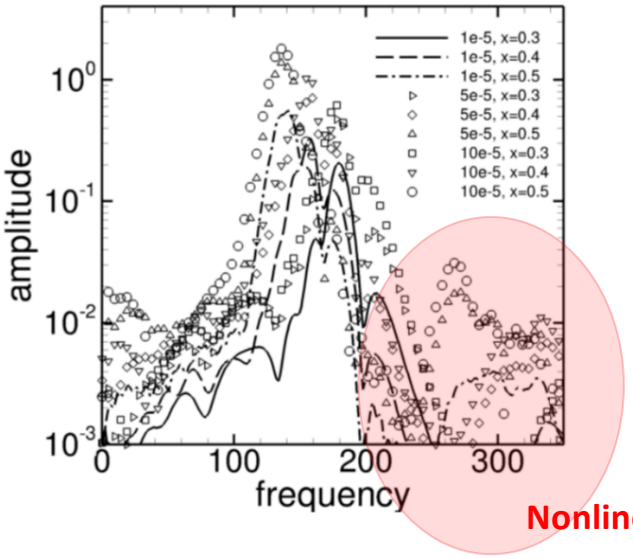

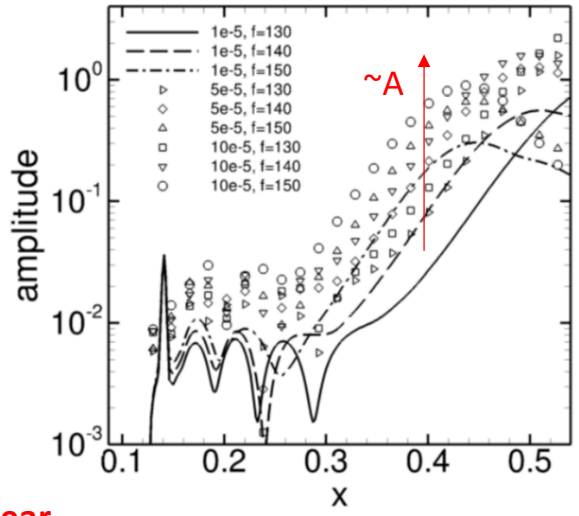

Fedorov (2013)

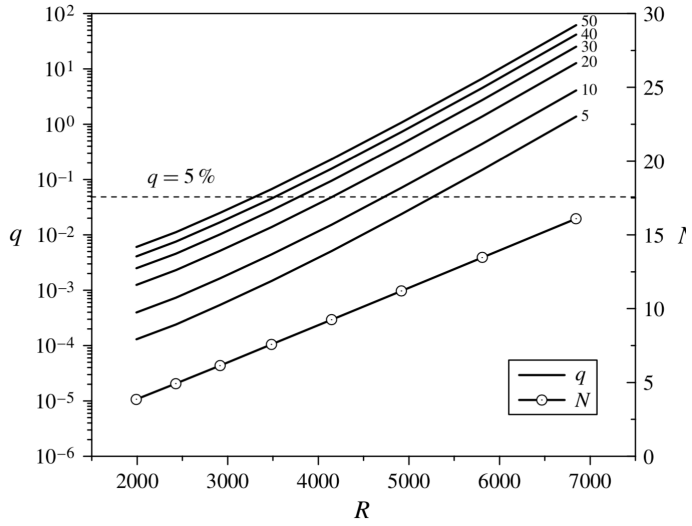

- As expected, larger particle size lead to vertical shift in amplitude curves
- In addition to higher disturbance amplitudes, a change in spectrum is observed
- Rough estimate for excitation frequency captures first peak in the spectrum (f ~ $v_p/2\delta_{99}$),

Effects of Particle Size

Pressure amplitude versus frequency for different particle sizes

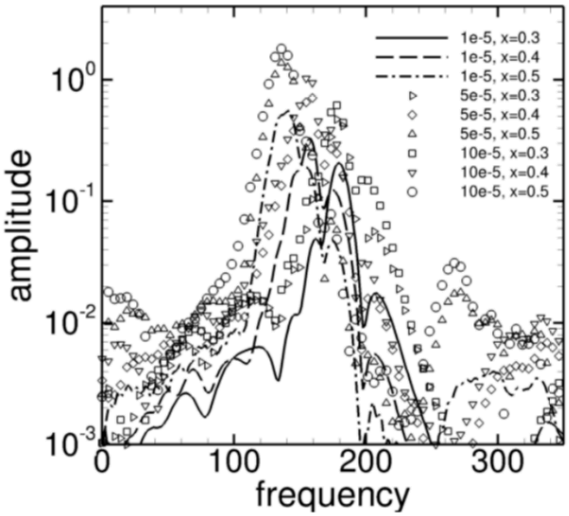

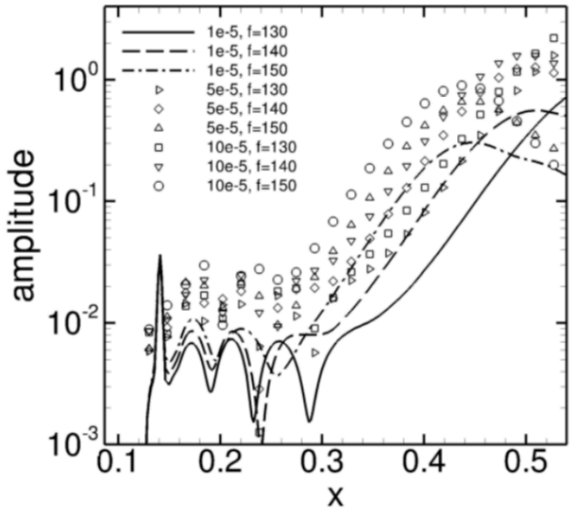

Estimate of excitation frequency

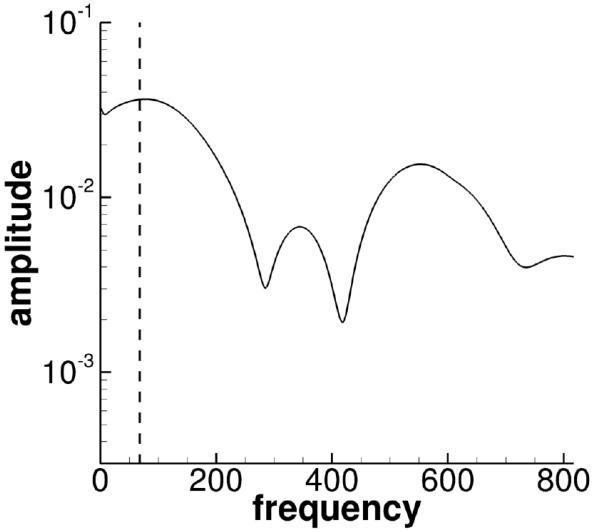

- As expected, larger particle size lead to vertical shift in amplitude curves
- In addition to higher disturbance amplitudes, a change in spectrum is observed
- Rough estimate for excitation frequency captures first peak in the spectrum ($f \sim v_p/2\delta_{99}$),

3D Flat Plate BL Particle Flow Simulation

3D Mach 5.35 Flat Plate Boundary Layer Flow

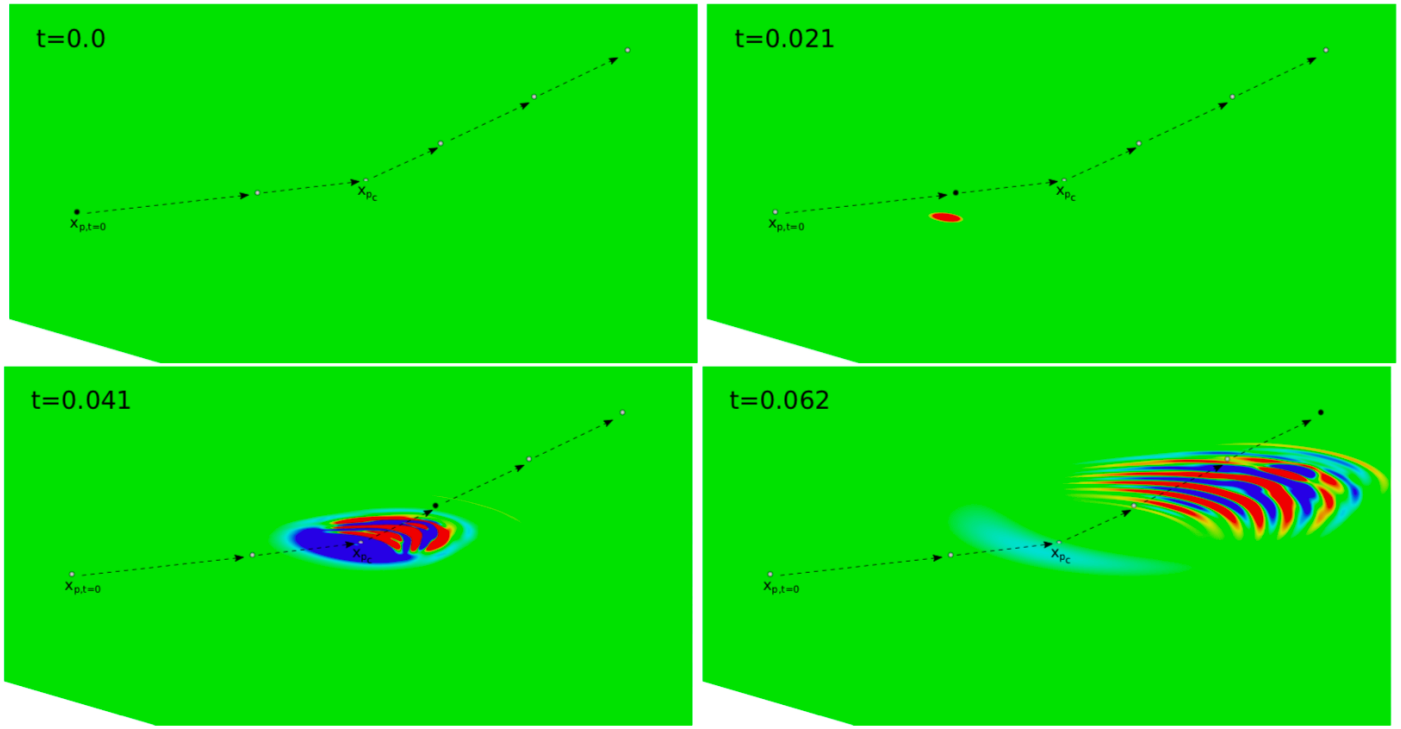

3D Flat Plate BL Particle Flow Simulation

Simulation Setup:
7° Wedge, Mach 6

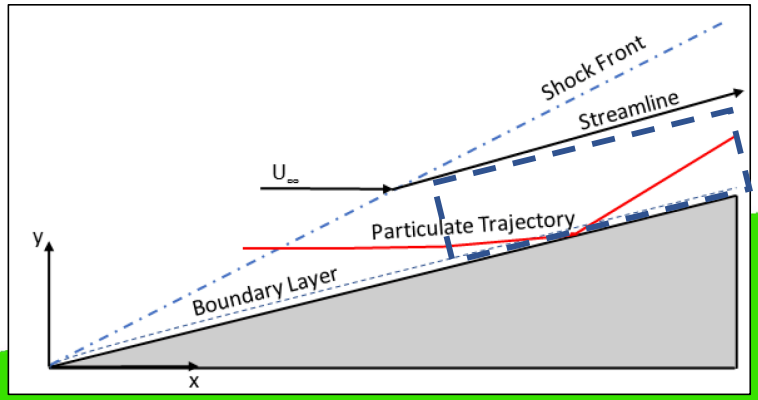

3D Flat Plate B-L Particle Flow Simulation

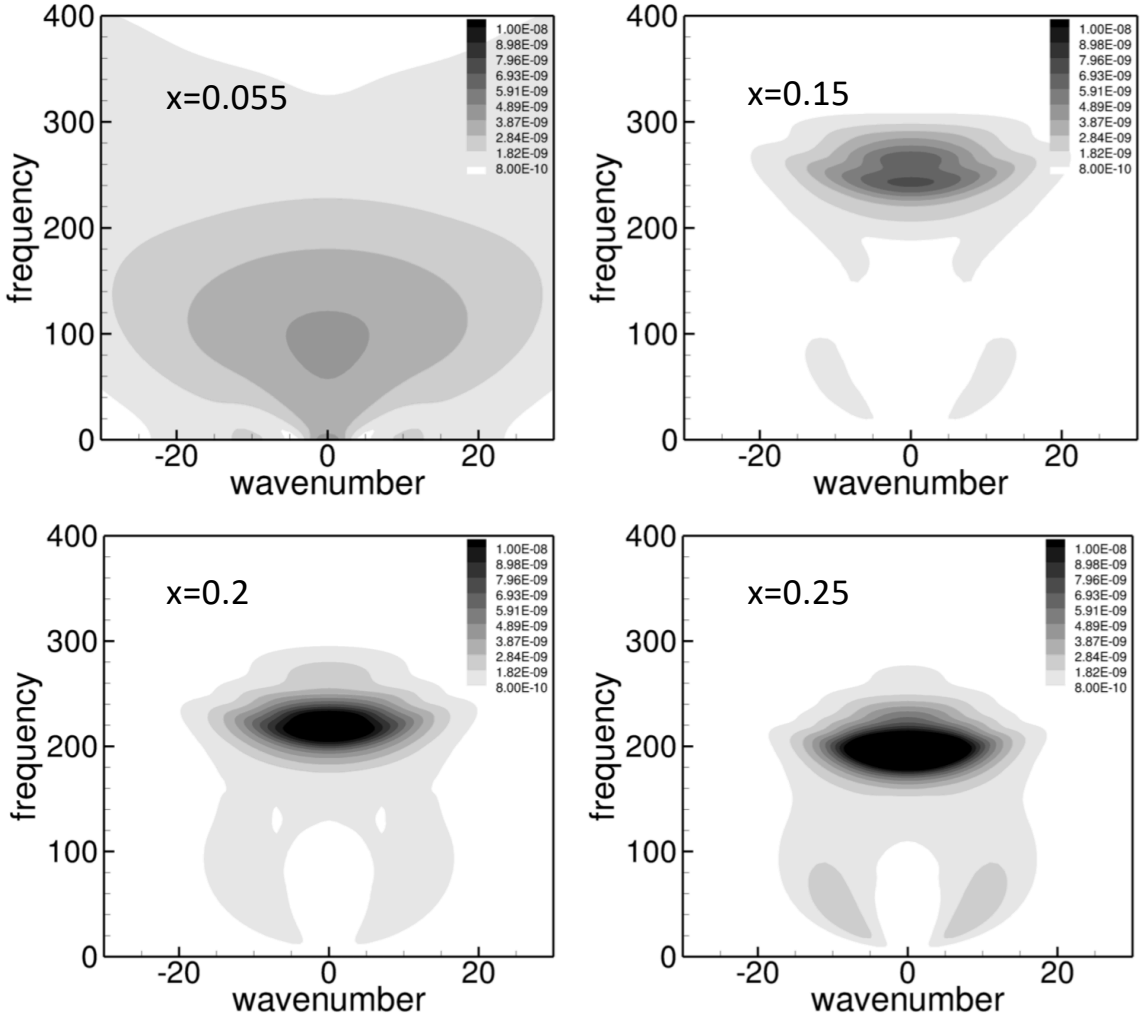

- Particulate collision with boundary-layer upstream of neutral curve,
- Frequency-wavenumber plots for various downstream locations,
- Wavepacket dominated by second mode 2D instability,
- Validated against wall-forcing simulations,

3D Flat Plate B-L Particle Flow Simulation

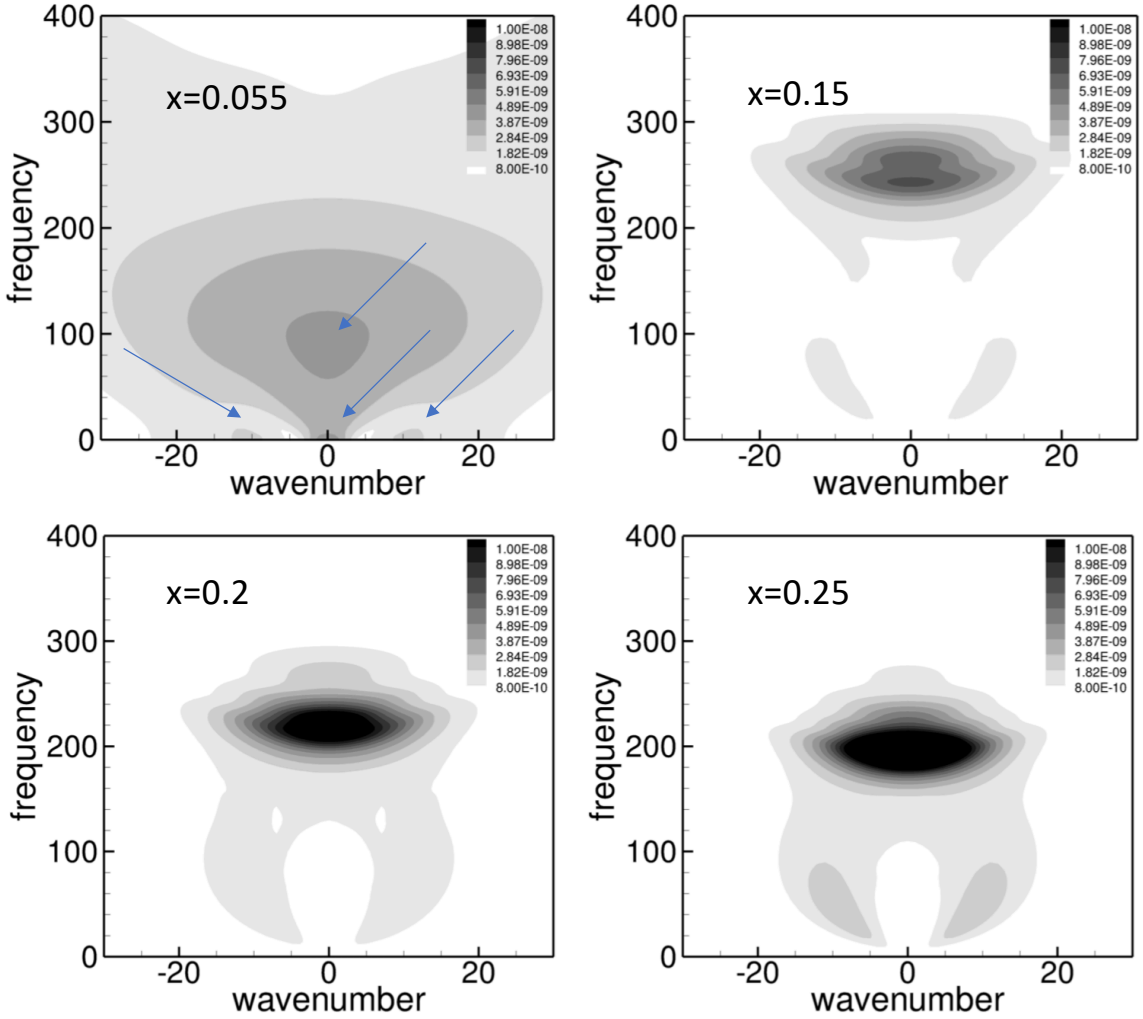

- Particulate collision with boundary-layer upstream of neutral curve,
- Frequency-wavenumber plots for various downstream locations,
- Wavepacket dominated by second mode 2D instability,
- Validated against wall-forcing simulations,

3D Flat Plate B-L Particle Flow Simulation

Sivasubramanian et al. 2016

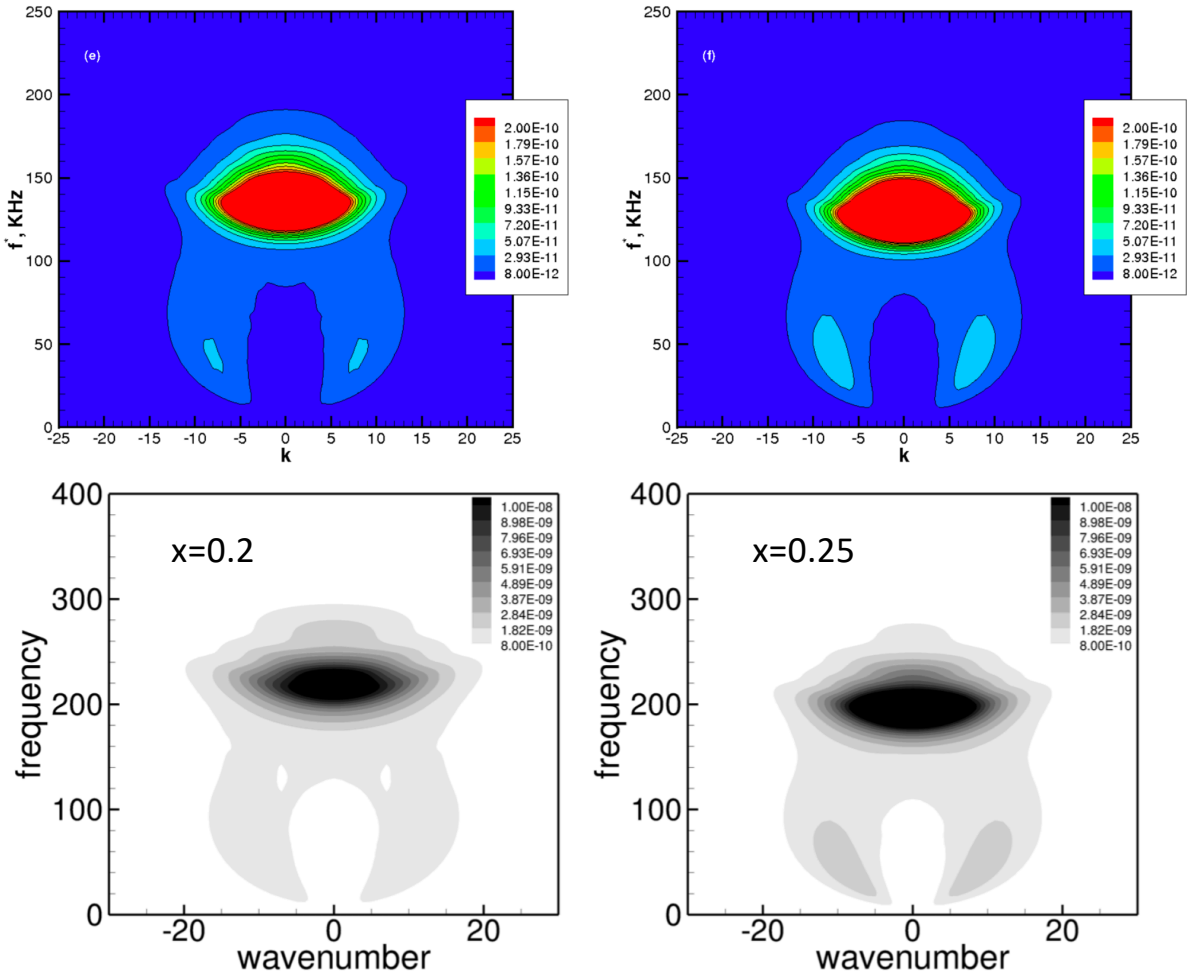

- Particulate collision with boundary-layer upstream of neutral curve,
- Frequency-wavenumber plots for various downstream locations,
- Wavepacket dominated by second mode 2D instability,
- Validated against wall-forcing simulations,

3D 14° Wedge Particle Flow Simulation

Flow conditions:

	14^o Straight Wedge
M_∞	4
$Re_\infty(1/m)$	7.381×10^6
$p_\infty(N/m^2)$	5530
$T_\infty(K)$	216.7
$U_\infty(m/s)$	1180.305

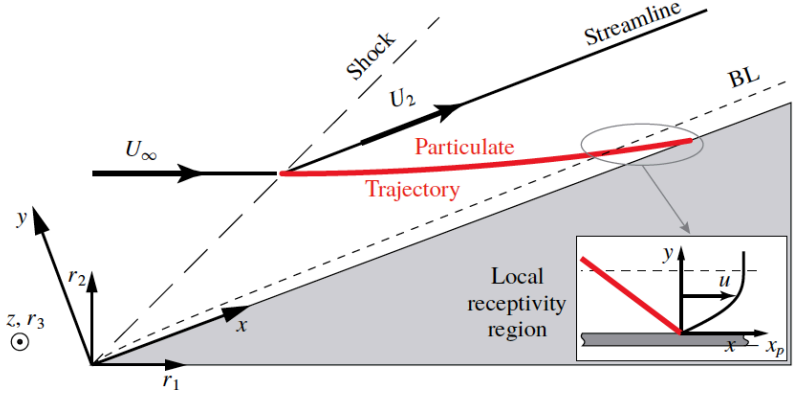

Adjusted from Churakov (2019)

- M=4 wedge flow is first mode dominated
- Comparison with Chuvakhov et al. (JFM 2019)
- **Chuvakhov et al. (2019) conclude that receptivity indifferent to particulate rebound**

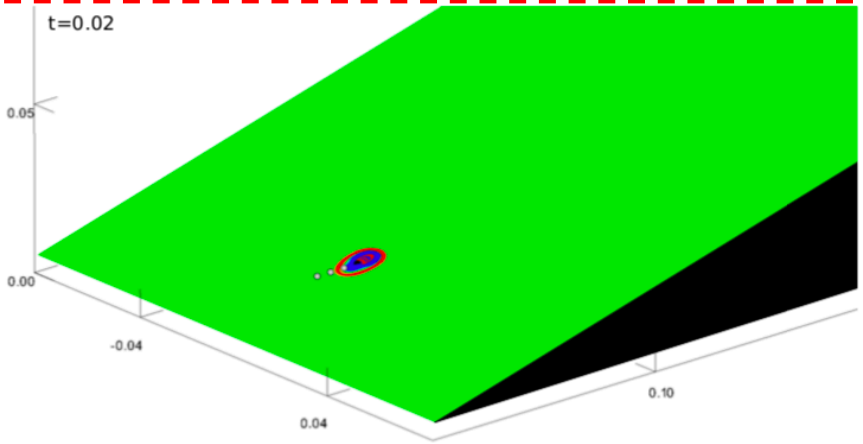

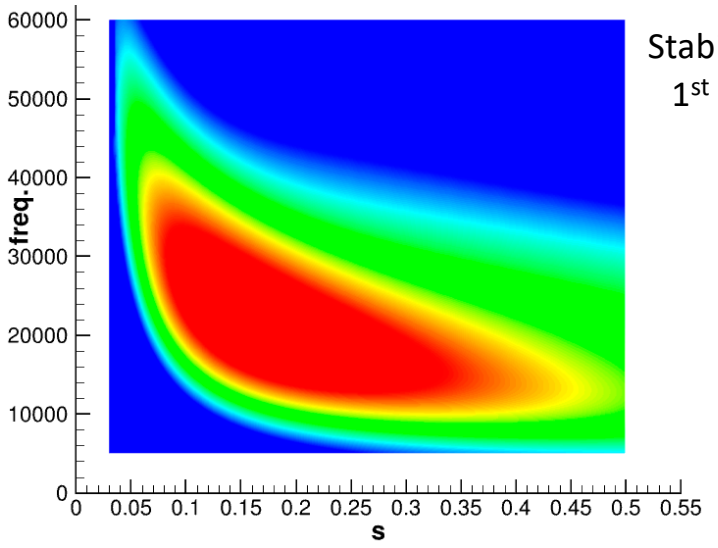

Stability Diagram for 1st Mode (β=474)

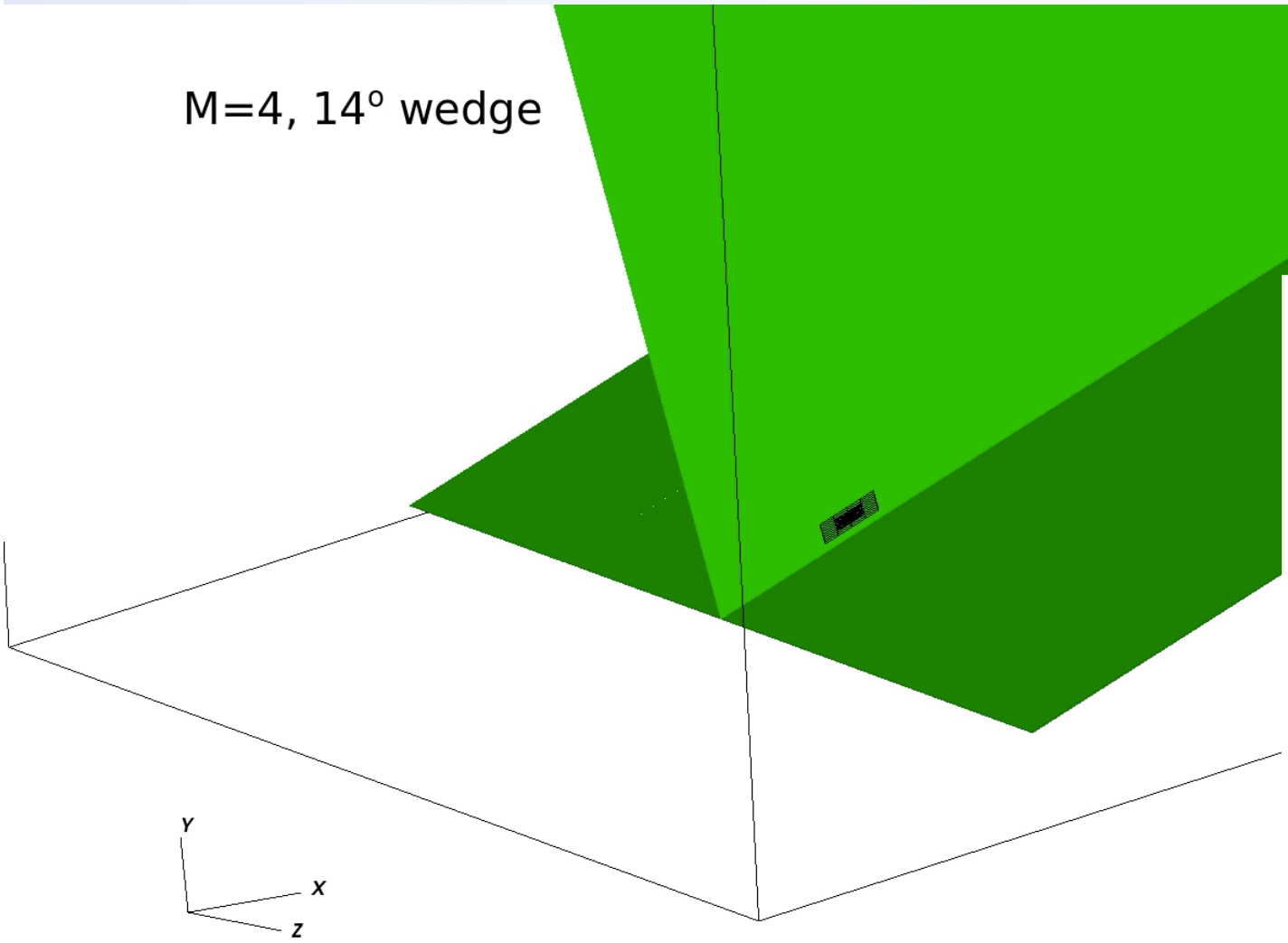

- AMR is ideal candidate for particulate induced transition simulations due to different scales that need to be resolved (e.g. *10μm* particle, 80 points, grid spacing of 0.125*μm* or 1.25 x 10^{-7})
- Greater resolution needed for computing particle trajectory than for resolving downstream wavepacket development,
- Grid levels can be removed after particle collision detected.

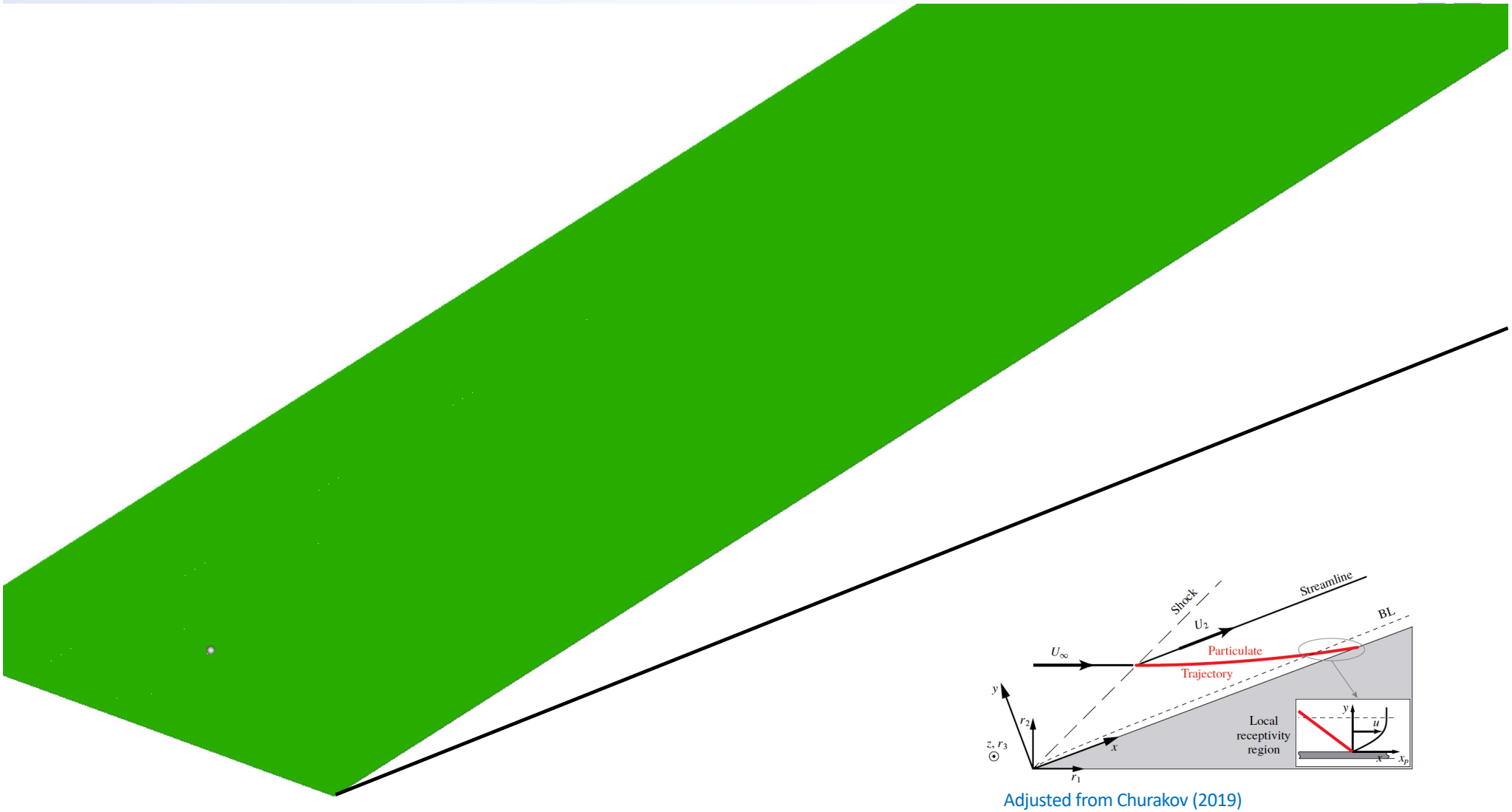

Adjusted from Churakov (2019)

3D 14^{o} Wedge Particle Flow Simulation

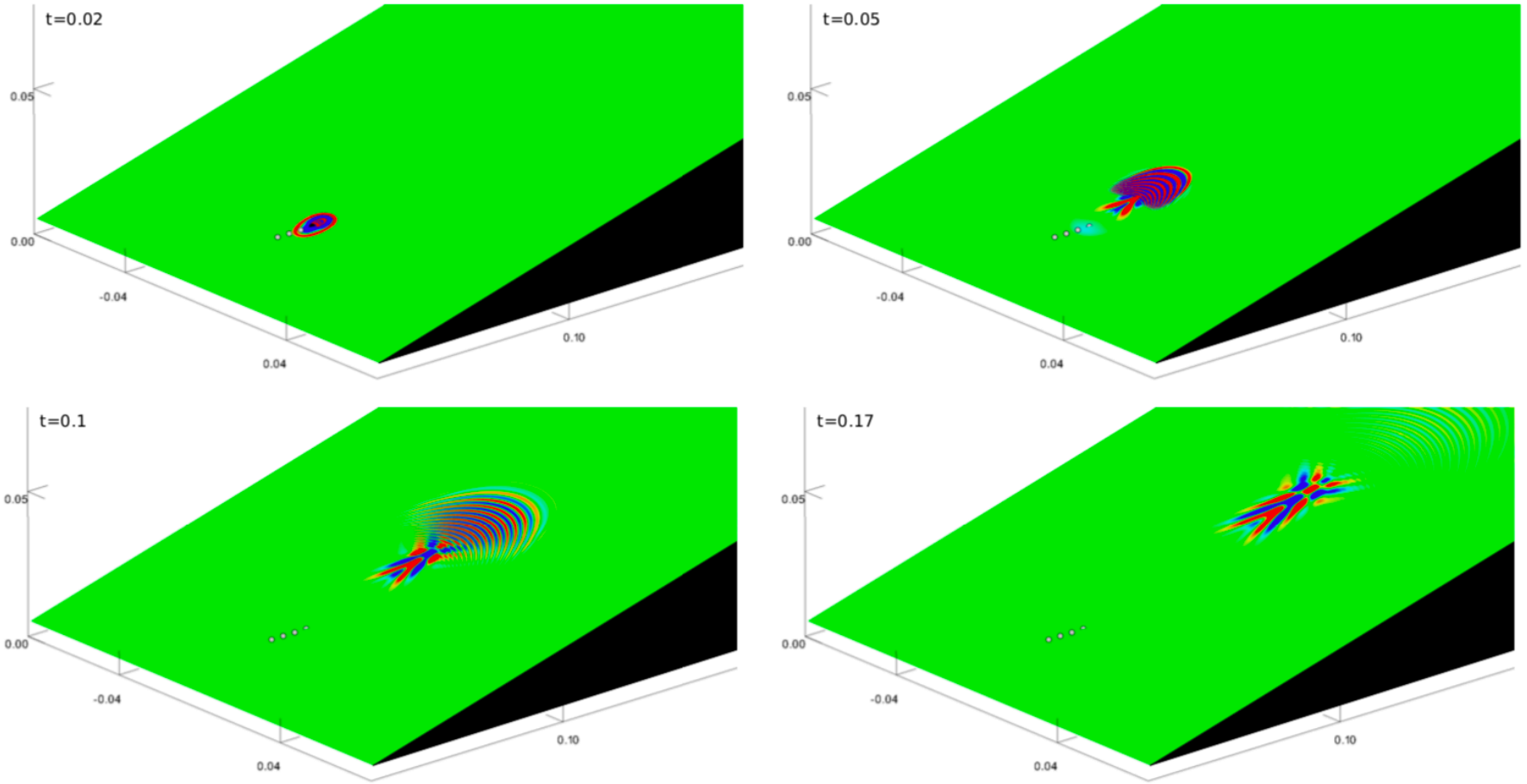

3D 14° Wedge Particle Flow Simulation

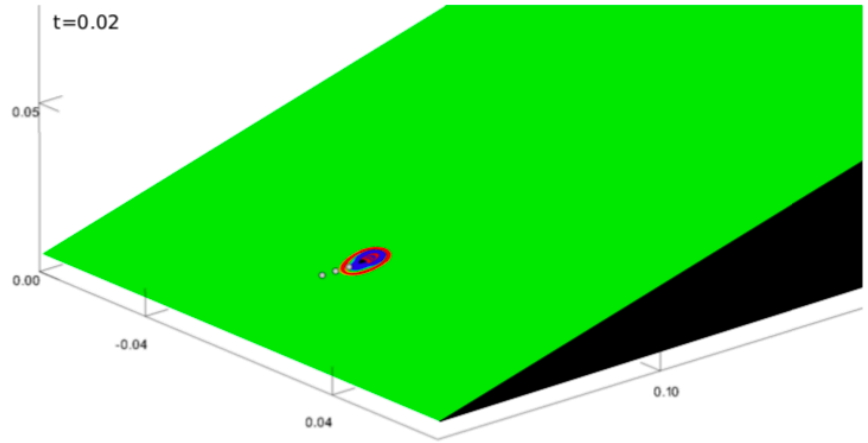

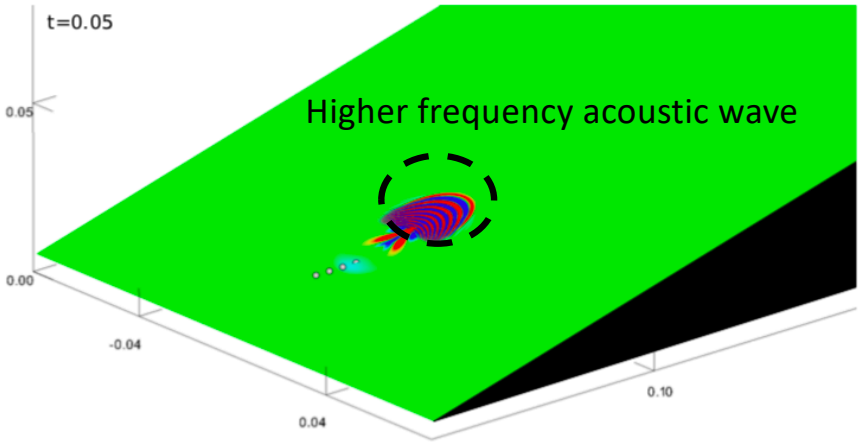

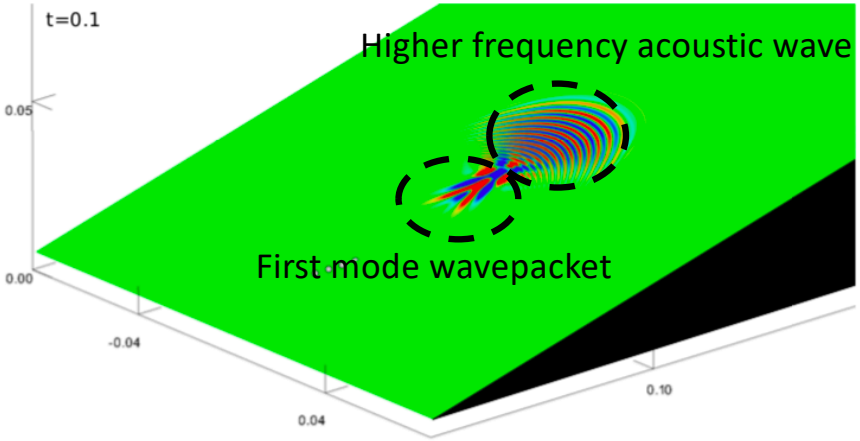

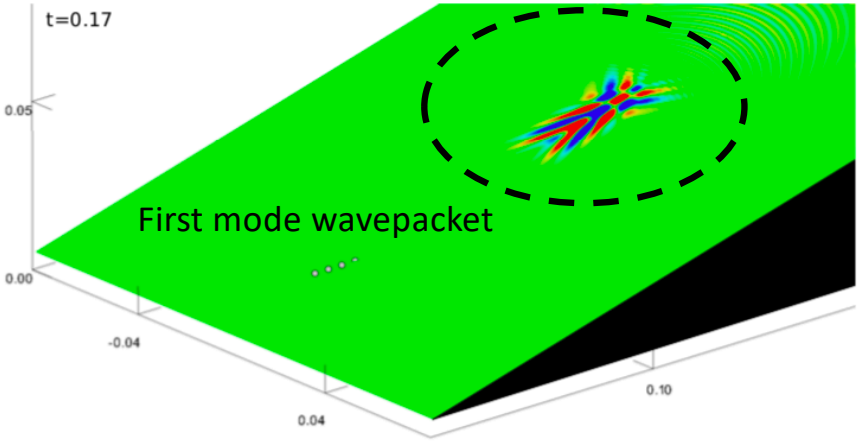

3D 14° Wedge Particle Flow Simulation

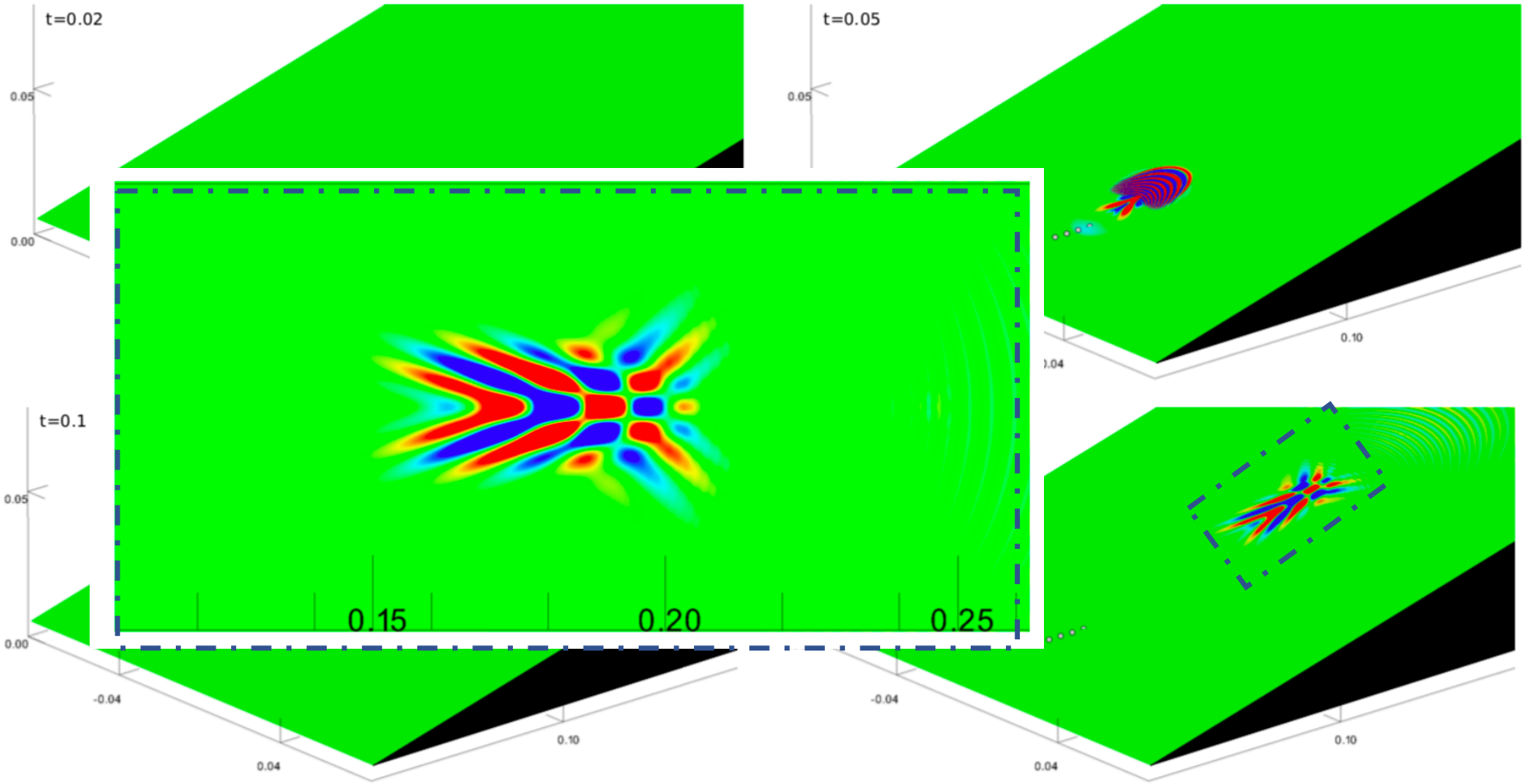

3D 14° Wedge Particle Flow Simulation

- β-ω diagrams

Just downstream of particle-impingement location

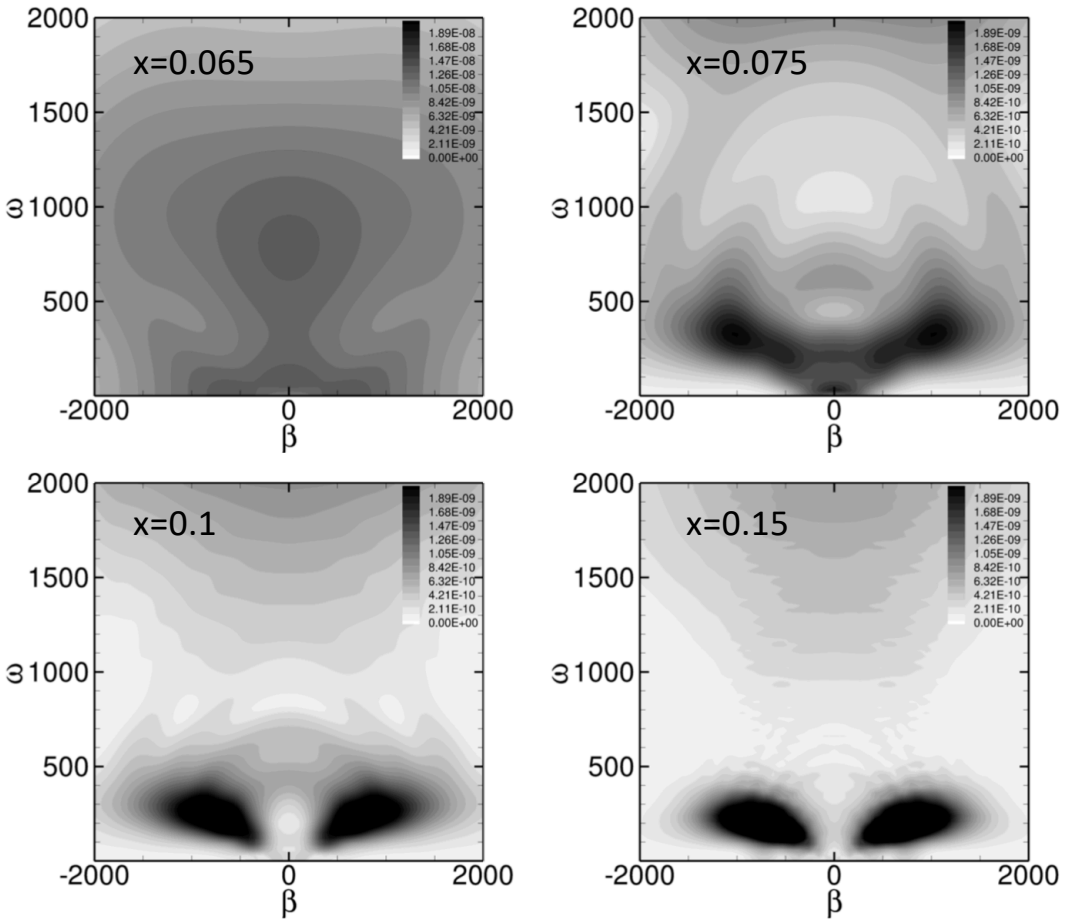

3D 14° Wedge Particle Flow Simulation

- β-ω diagrams

x=0.2

Current work - particle impingement

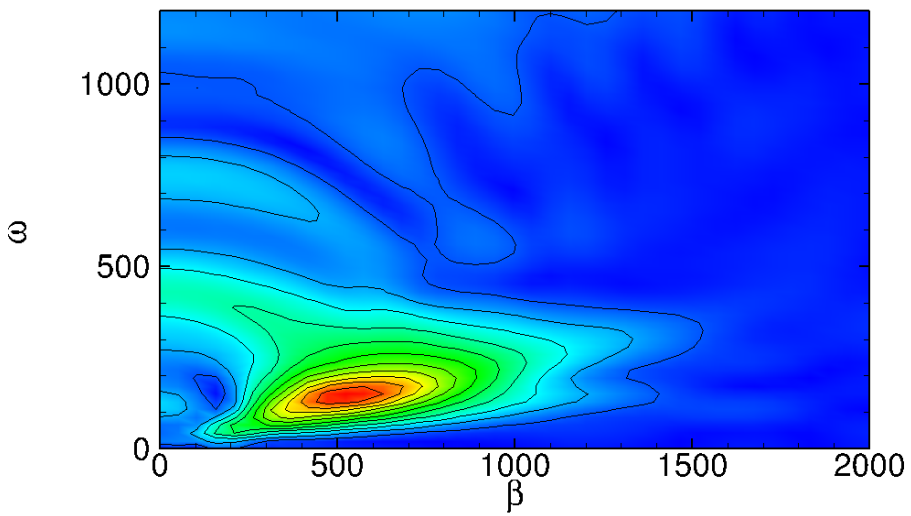

Chuvakhov et al. (2019)

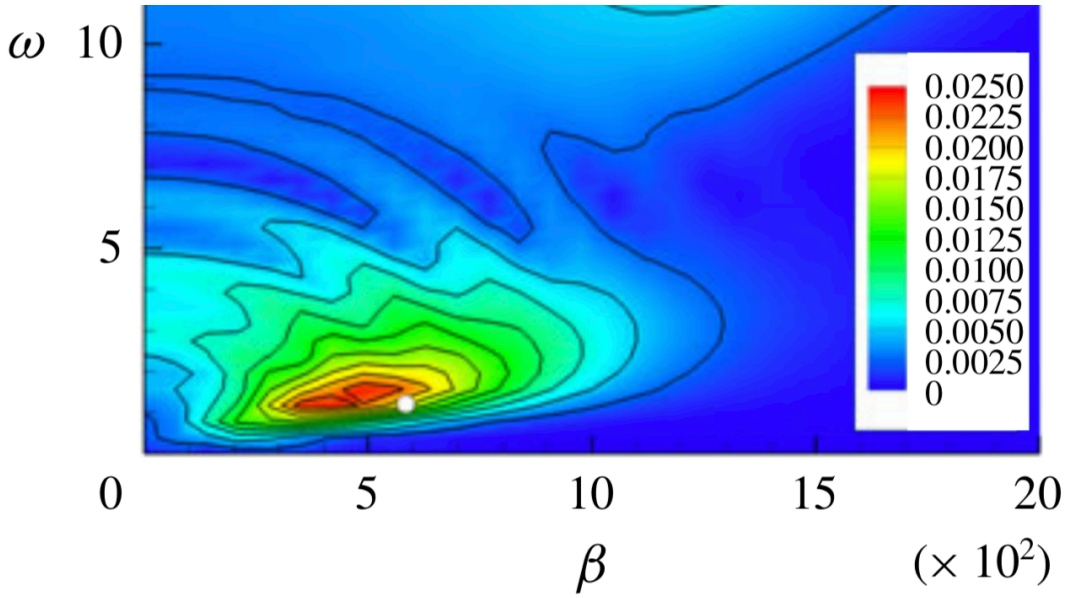

3D 14° Wedge Particle Flow Simulation

- β-ω diagrams

x=0.2

Current work – pulse disturbance

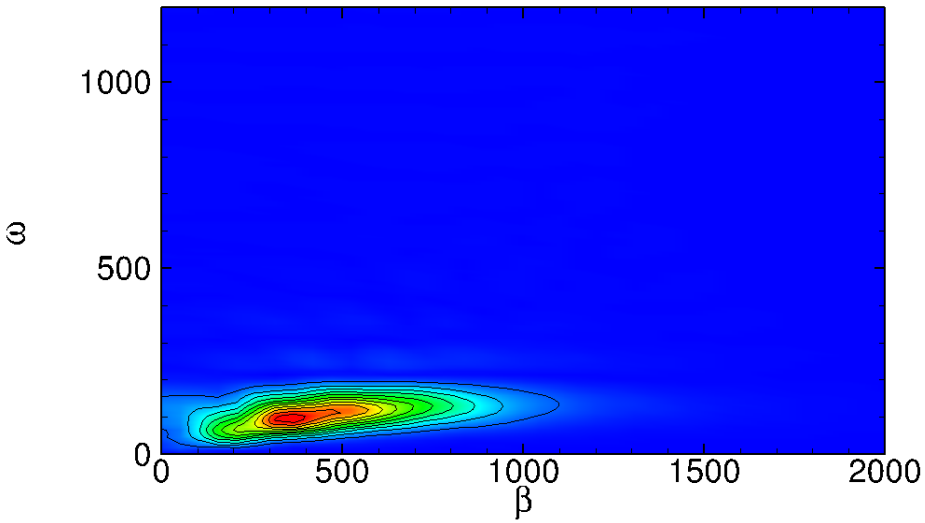

Chuvakhov et al. (2019)

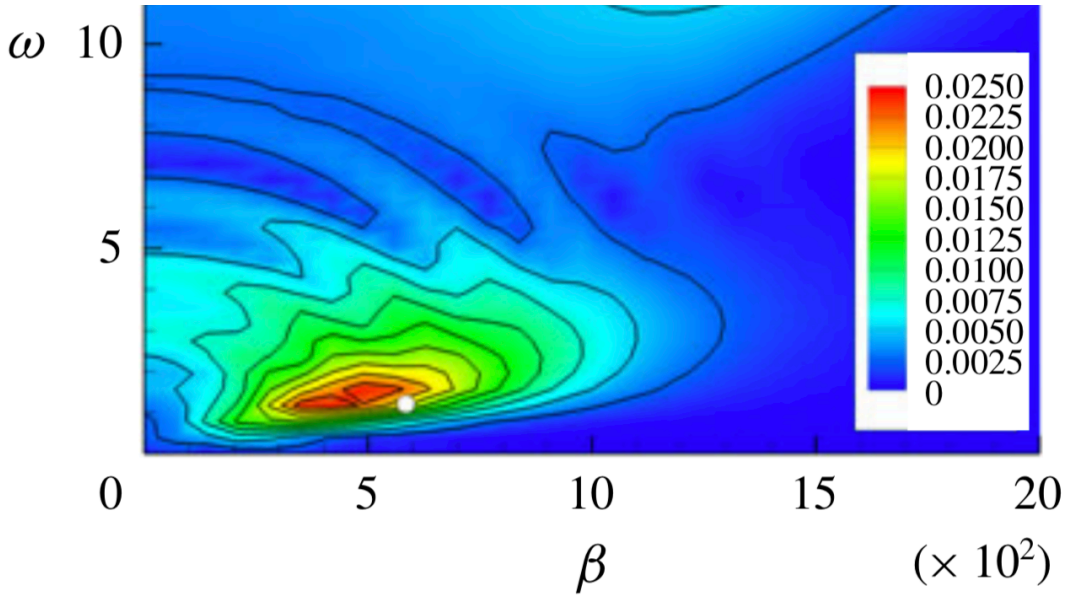

IB-based Particle Simulation

Immersed Boundary Methods: Motivation

- Why IBM Cartesian mesh methods?
  - Grid generation process can be fully automated
  - Cartesian mesh provides excellent numerical solution properties (although boundary operators can be problematic)
  - Higher-Order accuracy can be obtained in a straight-forward fashion for interior operators
  - Well-suited for exa-scale computing (data locality, tree-structure, *etc*.)
  - Fully-Eulerian solver approach for fluid-structure interaction problems (eliminating procedures for mesh deformation, transfer of solution from Ω^n to Ω^{n+1}, *etc*.)

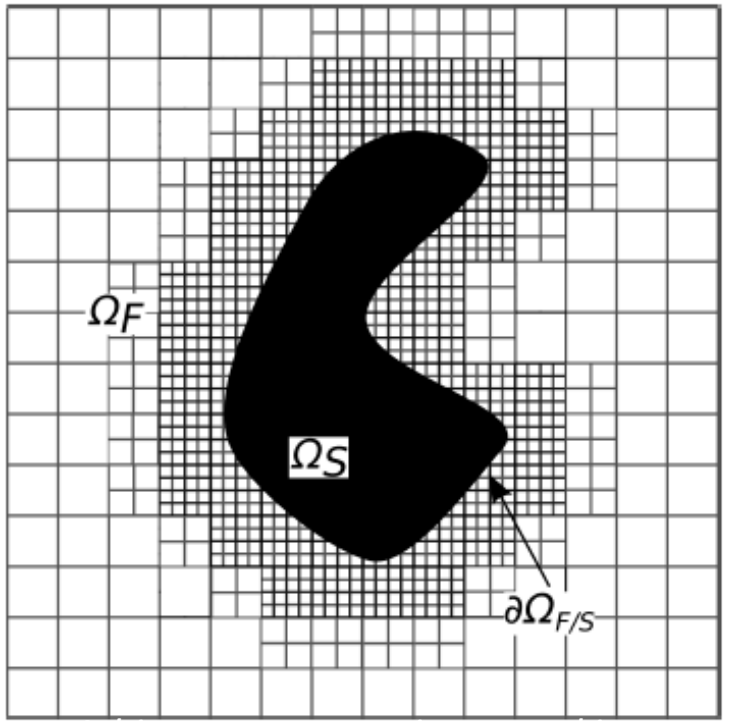

a Cartesian grid, where fluid and solid domains are marked with Ω_F and Ω_S, and immersed boundary as $\Omega_{S/F}$.

(Peskin et al. , Goldstein et al. , LeVeque and Li, Wiegmann and Bube, Linnick and Fasel, Johansen and Colella, Mittal and Iaccarino, Zhong, Duan et al., etc

IB-based Particle Simulation

Immersed Boundary Methods for NLDE: F-D stencil

- The forward-flux, **F+**, and the backward-flux, **F−**, are discretized with *n*th-order accurate **upwind-biased finite-differences** using centered grid stencils as proposed by Zhong (α determines degree of upwinding),

$$\left.\frac{\partial \phi}{\partial x}\right|_i = \sum_{k=i-n_s}^{i+n_s} c_k \phi_k - \alpha \overline{\Delta x} \left.\frac{\partial^{2n_s-1}\phi}{\partial x^{2n_s-1}}\right|_i,$$

c_k is the kth FD stencil coefficient

- Irregular grid point

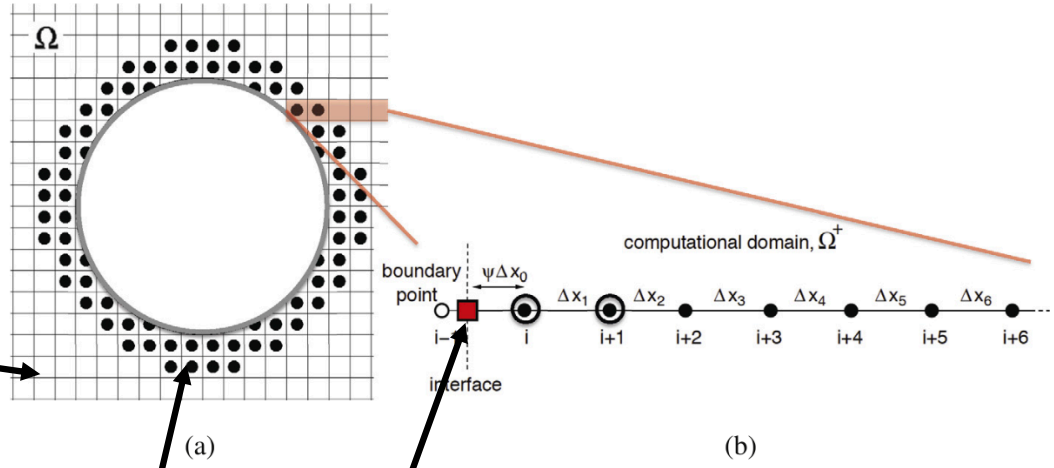

the boundary condition at immersed boundary

the backward-flux, **F−**, discretized for irregular stencil

$$\left.\frac{\partial \phi}{\partial x}\right|_k = c_{\partial\Omega}\phi_{\partial\Omega} + \sum_{m=1}^{p_k+1} c_{i+m-1}\phi_{i+m-1},$$

Brehm *et al*. (2015)

IB-based Particle Simulation

Non-Conservative Treatment of Viscous terms:

$$\frac{\partial \tau_{xy}}{\partial y} = \frac{d\mu}{dT}\frac{\partial T}{\partial y}\left(\frac{\partial u}{\partial y} + \frac{\partial v}{\partial x}\right) + \mu\left(\frac{\partial^2 u}{\partial y^2} + \frac{\partial^2 v}{\partial y \partial x}\right)$$

- In disturbance flow formulation:

  $\mu = \bar{\mu} + \tilde{\mu}, T = \bar{T} + \tilde{T}, u = \bar{u} + \tilde{u}, \& \; v = \bar{v} + \tilde{v}$

- avoids computing baseflow derivatives after interpol
- showed higher accuracy than conservative approach
- all derivatives are computed directly:

  first and second derivatives

$$\left.\frac{\partial \phi}{\partial x}\right|_k = c_{\partial\Omega}\phi_{\partial\Omega} + \sum_{m=1}^{p_k+1} c_{i+m-1}\phi_{i+m-1} + O(\Delta x^{2n})$$

  mixed derivatives

$$\left.\frac{\partial^2 \phi}{\partial x \partial y}\right|_{i,j,k} = c_{\partial\Omega}\phi_{\partial\Omega} + \sum_{m=1}^{n_R-1+n_A} c_{i_m,j_m,k_m}\phi_{i_m,j_m,k_m} + O(\Delta x^{2n})$$

Point Cloud for Derivative Computation

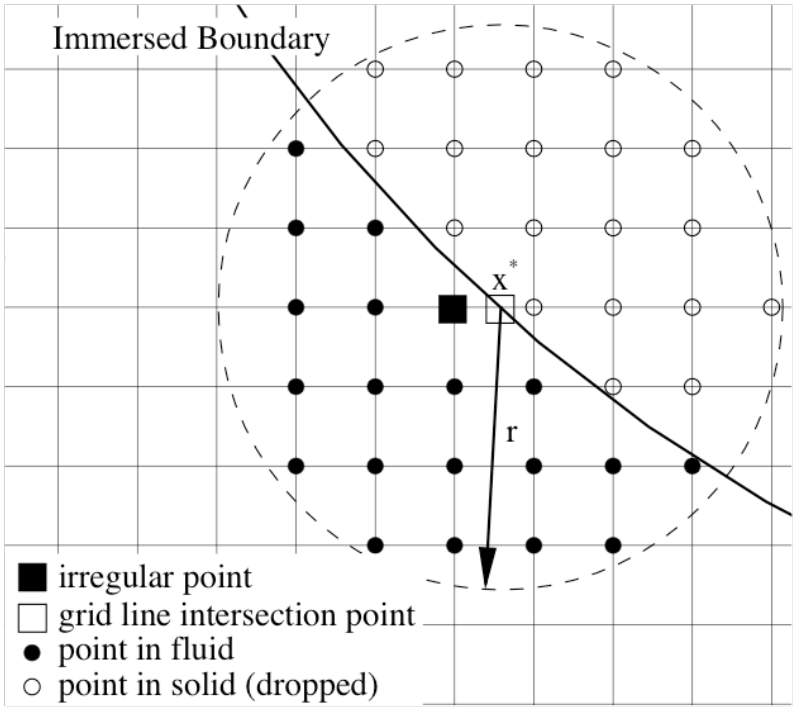

IB-based Particle

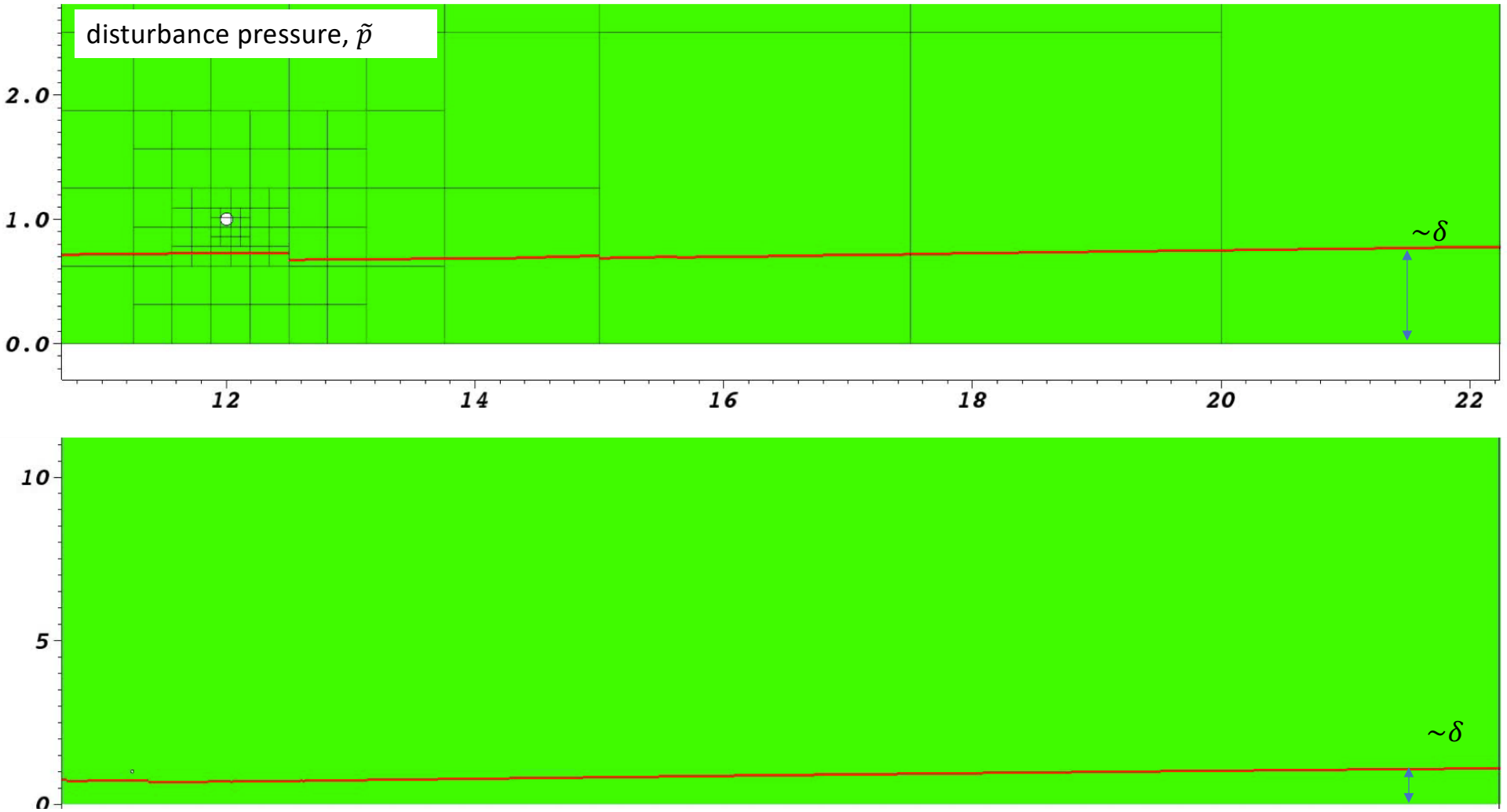

IB-based Particle

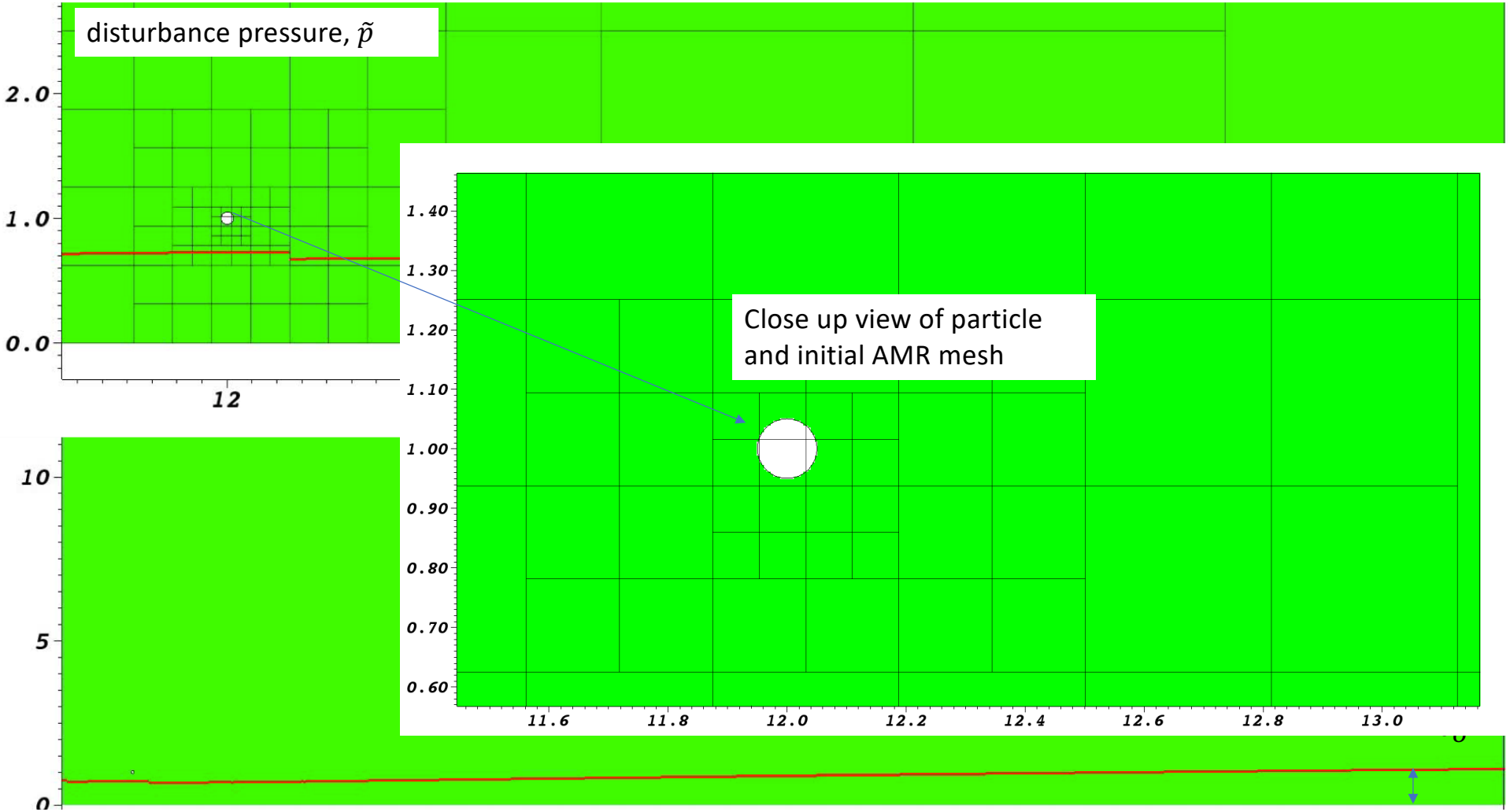

IB-based Particle

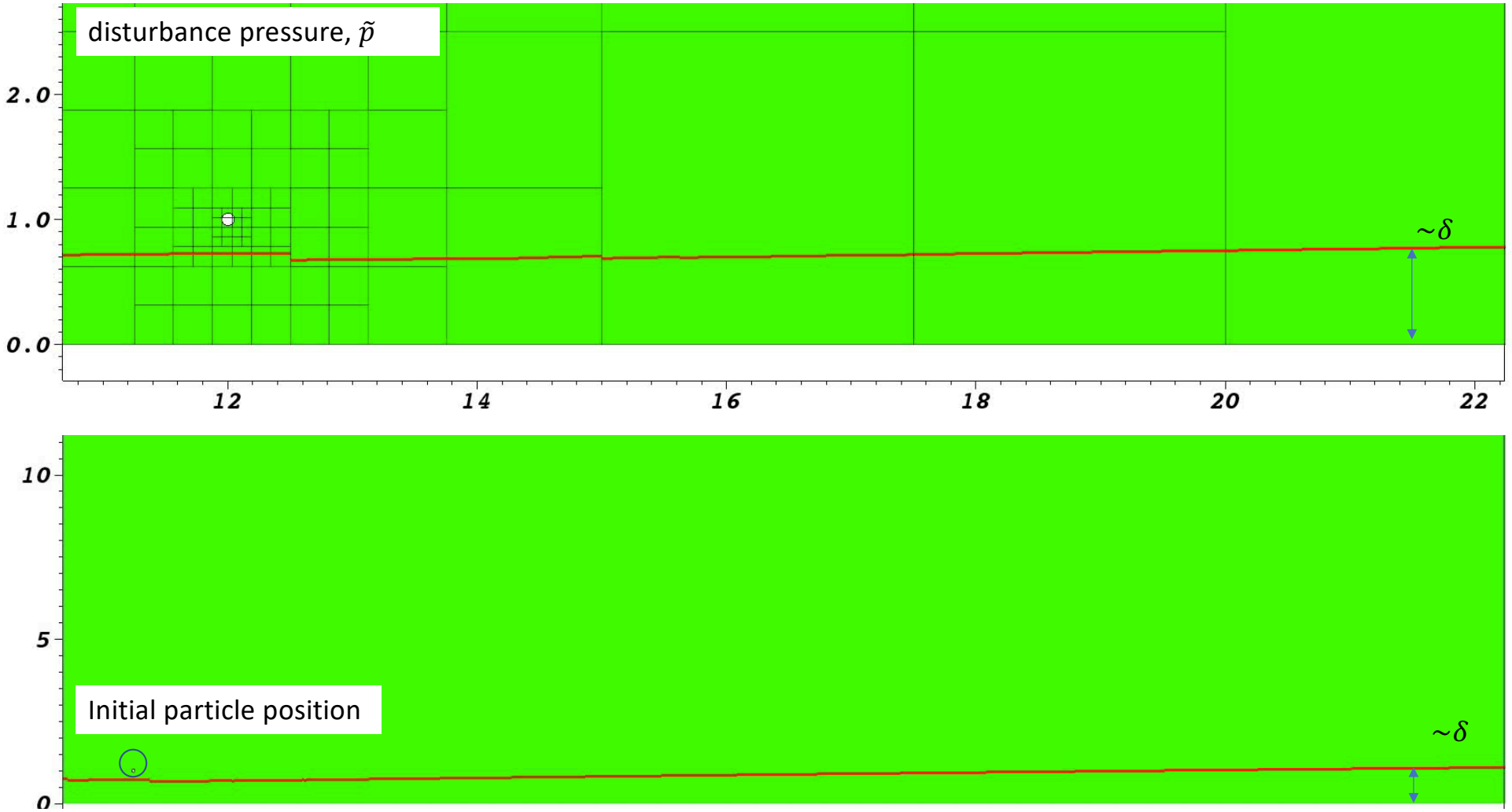

Outline

Particle Flow Simulations Background

Background, prior research and findings.

Numerical Methods

BitCart, Dual-Mesh Approach, and AMR.

Simulations Results

Validation, and 2D/3D patricle flow simulations results.

Summary, Outlook, & Research Interest

Summary of presented research

“Towards Fully-Resolved Particulate-Induced Transition Simulations for High-Speed Boundary-Layers with an Immersed Boundary Method”, O. M. F. Browne, S. M. A. Al Hasnine and C. Brehm, AIAA SciTech, Orlando, Jan 2020

Summary and Outlook

- Developed efficient approach for particle-flow interaction simulations,
- Particle-impingement considering different sizes and forcing locations,
- Predominantly linear receptivity process (depends on flow condition),
- Results potentially indicate that particle impingement is difficult to model considering a simple pulse when the disturbance is introduced downstream of the neutral curve,
- Moved to a higher fidelity approach by modeling the particle with an immersed boundary approach,

Summary, Outlook & Research Interests

Thank you for listening.

Any questions or comments?